# Non-Epitaxial Carrier Selective Contacts for III-V Solar Cells: A Review

Vidur Raj [*], Hark Hoe Tan[*] and Chennupati Jagadish[*]

[1]Department of Electronic Materials Engineering, Research School of Physics, The Australian National University, Canberra, ACT 2601, Australia

vidur.raj@anu.edu.au; hoe.tan@anu.edu.au; chennupati.jagadish@anu.edu.au

**Abstract**

In the last few years, carrier selective contacts have emerged as a means to reduce the complexities and losses associated with conventional doped p-n junction solar cells. Still, this topic of research is only at its infancy for III-V solar cells, in comparison to other solar cell materials such as silicon, perovskites, chalcogenides, etc. This could be because high quality III-V solar cell materials can be achieved relatively easily using epitaxial growth techniques such as MOCVD and MBE. However, current epitaxial III-V solar cells are very expensive and cannot compete for the terrestrial market, and therefore, researchers are developing alternative growth methods such as thin-film vapor–liquid–solid (TF-VLS), hydride vapor phase epitaxy (HVPE) and closed space vapor transport (CSVT), which are significantly lower in cost compared to epitaxial III-V solar cells. However, at present, these relatively nascent low cost growth methods, face severe optimization issues when it comes to growth of controlled p-n junction, along with heavily doped window and back surface field layers. In such cases, carrier selective contacts can be hugely beneficial. In this review, we cover some of the most recent research on the use of carrier selective

contacts for III-V solar cells. Future prospects, challenges, and new device concepts using carrier selective contacts will also be discussed.

***Keywords:*** *carrier selective contact, III-V solar cell, passivation, heterojunction, window layer.*

## 1. Introduction

Silicon is by far the most popular material for the terrestrial PV market [1]. Though silicon solar cells have achieved remarkable success in the commercial market, it is not an optimum material for light harvesting because of its indirect bandgap. Silicon solar cells require a thickness higher than a hundred micron to achieve sufficiently high absorption. In comparison, III-V materials such as InP and GaAs are a very efficient absorber of light and can absorb most of the visible spectrum within 2-3 microns [2, 3]. This thickness can further be reduced by the utilization of a back reflector or a Lambertian surface [4-7]. Thinner cells not only lower the cost but also allow for the fabrication of flexible solar modules, which can find new applications in the areas of integration with cloth/fabric, electronic skin, lightweight systems, and internet of things [8].

At present, most of these III-V thin film cells are grown using metal-organic chemical vapor deposition (MOCVD), which is an expensive technique and requires relatively costly infrastructure, substrates, gases, and precursors [9, 10]. Kelsey et al. report that current III-V solar module prices can often exceed $150/W, which is roughly 400X the current prices for mainstream c-Si solar and cadmium telluride (CdTe) modules ($0.30–$0.50/W) [9]. It has been proposed that unless there is a radical change in the growth methodology [9, 11], III-V solar cells cannot compete in the terrestrial market. Thereby, researchers are developing new low-cost III-V growth techniques, which can replace relatively costly MOCVD/MBE techniques. Some of the new growth techniques include TF-VLS (Thin Film – Vapor Liquid Solid)[12-14], close-spaced vapor transport (CSVT)[15-18], Aerotaxy [19-21], and nanowire heteroepitaxy [22-25]. These growth

techniques have shown enormous promise towards a significant reduction in the cost of III-V solar cells. A review of low-cost growth of III-V materials can be found in reference [26].

Though these low-cost techniques have shown tremendous promise, there are still several challenges which need addressing before their implementation on a commercial scale such as: (a) formation of a controlled p-n junction, (b) uniform and controlled doping, (c) lattice-matched window layer and back surface field (BSF) layer growth, and (d) low minority carrier lifetime [17, 21, 26, 27]. The problem is further complicated when a window or BSF layer needs to be doped while maintaining a relatively low interface recombination velocity [26]. Optimization of growth conditions to simultaneously tackle these challenges can often be cumbersome, if not impossible. Also, most of these challenges exist because, for III-V solar cells, the research community is still reliant on the conventional architecture, which includes a p-n junction, a window layer, and a BSF layer followed by a contact layer. A more novel approach would be to utilize non-epitaxial carrier selective contacts to eliminate the need for the doped p-n junction, window, and BSF layers.

For low-cost growth techniques, these doped junctions are not only limited by practical difficulties but may also lead to several optoelectronic losses, some of which are listed in table 1. Furthermore, in recent years, it has become clear that the doped p-n junction or BSF/emitter layer is not necessary for the operation of a high-efficiency solar cell [28]. Carrier selective contacts have emerged as a cost-effective, yet efficient alternative to these doped junctions [28]. Today, almost all high-efficiency solar cells utilize carrier selective contacts in one form or other [29-31]. In fact, even high-efficiency III-V solar cells incorporate an emitter layer and a BSF layer, which are a form of carrier selective layer [28, 32].

To overcome the limitations of low-cost growth techniques, what we need is a solar cell that does not rely on epitaxial p-n homojunction or window layer or BSF for high performance. Currently,

the best alternative to simultaneously solve all of these problems is the utilization of carrier selective contacts. The purpose of this review is to provide an overview of different inorganic and organic materials that have been used as carrier selective contacts for InP and GaAs solar cells. The review starts with a short discussion on passivation and carrier selectivity followed by a detailed review of electron selective contact (ESC) and hole selective contact (HSC). While discussing ESC and HSC, we include most of the recent results, and wherever necessary, we also discuss some of the earlier results on heterojunction solar cells based on InP and GaAs. After a broad review of carrier selective contacts, we discuss the future prospects and new possibilities of III-V solar cells using carrier selective contacts.

**Table I:** Different optoelectronic losses associated with the doping of solar cells

| **Type of Loss** | **Issue** | **End Result** |
|---|---|---|
| Optical | Parasitic free carrier absorption<br>Parasitic absorption in the window layer | Reduced $J_{sc}$ |
| Recombination Loss | Auger Recombination<br>SRH | Reduced $V_{oc}$ |
| Transport Loss | Resistive Loss | Reduced FF |
| | Low diffusion Length | Reduced $J_{sc}$ |

## 2. Passivating Contact vs. Carrier Selective Contact

Frequently, the passivating layer and carrier selective contacts are used synonymously without any real distinction. Ideally, a carrier selective contact is also expected to act as a passivation layer, and vice-versa; however, both are not the same. In fact, a significant amount of work on high-efficiency silicon solar cells shows that a separate high-quality passivation layer is required in addition to a carrier selective contact to achieve high efficiency [29, 33, 34]. In cases where a carrier selective contact also acts as a passivation layer, it should be referred to as a passivating carrier selective contact [35]. In general, the effectiveness of a passivation layer is measured in terms of surface recombination velocity (SRV), whereas the efficacy of a carrier selective contact is measured in terms of the ratio of conductivity of majority to minority carriers [36]. In other words, the aim of using a passivation layer is to achieve as low SRV as possible, whereas the aim of using a carrier selective layer is to achieve as high asymmetric conductivity of carriers as possible. In subsequent sub-sections, we briefly discuss the fundamental aspects of passivation and carrier selectivity.

### 2.1 Passivation

At the semiconductor surface, abrupt termination of crystal lattice leaves a large number of electronically active, unsaturated, broken bonds (“dangling bonds”), which introduce energy states within the forbidden bandgap of the semiconductor [35]. Such energy states (called “surface states”) are a very effective mediator of non-radiative recombination and can cause severe degradation to overall solar cell performance [37]. The minimization of non-radiative recombination through these electronically active surface states is known as surface passivation [37, 38]. Surface passivation can be achieved either through covalent bonding (chemical passivation) of surface atoms or through interface charge carrier population control (sometimes

also referred to as “field-effect passivation”) [35, 38-40]. Chemical passivation or passivation through covalent bonding is often accomplished by the application of a thin (passivation) layer of another semiconductor or an insulator on the semiconductor surface. For effective chemical passivation, the passivation layer must form a stable covalent bond with the surface atoms of the semiconductor, such that the interface defect density is significantly lower than the surface defect density, and bulk recombination within the passivation layer is also very low [35, 38-40]. In addition to the deposition of a passivation layer, there are other ways in which chemical passivation can be achieved, such as, plasma treatment, sulfurization, thermal oxidation, nitridation. [41-44]

Another approach to surface passivation is through interface carrier population control, which relies on the fact that there is a requirement of both electrons and holes for recombination through surface defect states [35]. Therefore, if the concentration of either electrons or holes is reduced significantly at the interface, interface recombination also reduces. When the reduction of electrons or holes at the interface is achieved through a built-in electric field, it is known as “field-effect passivation”. The best example of passivation through carrier population control is the back surface field, where heavy doping is used to reflect the minority carriers. An excellent review on this topic can be found in ref [35]. Often both chemical passivation as well as interface carrier population control, are used in conjunction with each other to achieve maximum reduction in surface recombination.

In general, III-V solar cells are grown using MOCVD (Metal-Organic Chemical Vapour Deposition) or Molecular Beam Epitaxy (MBE), and excellent surface/interface passivation can be achieved by utilizing a lattice-matched III-V alloy (called “window layer”). For example, an SRV as low as 1.5 cm/s has been achieved for $Ga_{0.5}In_{0.5}P$/GaAs interface [45]. However, the current review is mainly about III-V solar cells where deposition of lattice-matched window layers

can be complicated because of the requirement of precise control of composition; therefore, we confine ourselves to examples of non-epitaxial passivation layers. For both GaAs and InP, many different non-epitaxial materials have been investigated for passivation. Some of these include but are not limited to $Al_2O_3$, $Gd_2O_3$, $LaF_3$, MgO, $Ta_2O_3$, $SiO_2$, $P_2O_5$, $Si_3N_x$, ZnO, ZnS, GaS, etc [46-53]. For some of these oxides/III-V interfaces, defect density as low as $10^{10}$ $cm^{-2}eV^{-1}$ has been achieved [47, 54]. In particular, there are many reports on deposition of metal oxides for high-quality III-V defect passivation for MOSFET applications [46, 48, 55, 56] that can also be implemented to III-V solar cells. Passivation of III-V materials using non-epitaxial techniques have widely been reviewed for different applications and can be found in references [46, 49, 55-66]. In addition to the deposition of a passivation layer, several kinds of chemical and physical techniques have also been used for III-V passivation. For example, sulfur treatment of GaAs and InP surfaces has resulted in high-quality passivation [49, 61, 67-71]. Similarly, hydrogen [72, 73] and sulfur plasma [74] treatments have shown effective passivation for both InP and GaAs.

### 2.2 Carrier Selectivity

In contrast to passivation, carrier selectivity requires asymmetric conductivity toward electrons and holes, i.e., an electron (hole) selective layer should be highly conducive to electrons (holes), while maintaining a high resistivity to holes (electrons). Though a selective contact should ideally be passivating, it is not a necessary condition to be a carrier selective contact. In fact, almost all high-efficiency solar cells use separate layers for passivation and carrier selectivity. To be an efficient carrier selective contact, the material should be (a) wide bandgap, (b) heavily n-type or p-type dopable, (c) capable of forming asymmetric band off-set with the absorber, and (d) able to achieve low contact resistance. In general, low work function materials are employed as electron selective contact, whereas, high work function materials are used as hole selective contact. A good

carrier selective contact is often characterized by low dark current density, $J_0$, and low contact resistivity. Therefore, an easy way to define selectivity, S is in terms of minority carrier dark current density ($J_0$), contact resistance ($\rho_c$) and thermal voltage ($V_T$) as follows [36]:

$$S = V_T / J_0 \rho_c$$

Furthermore, often to achieve a small $J_0$, researchers employ carrier selective contact in a small area and introduce passivation in the rest of the solar cells. Some of the recent reviews and theoretical works on carrier selective contacts can be found in reference [1, 33, 35, 39, 40, 75-78]

## 3. Window Layer

Conventional III-V solar cells utilize wide bandgap, lattice-matched, and heavily doped window layers for passivation of front and back surface, while also minimizing the contact recombination [79]. Therefore, we review III-V window layers before moving onto carrier selective contact. GaAs has hugely benefitted from the availability of a wide range of lattice-matched window layers such as $Al_xGa_{1-x}As$, $Al_{0.5}In_{0.5}P$, $Ga_{0.5}In_{0.5}P$, and $(Al_xGa_{1-x})_{0.5}In_{0.5}P$, which also have a larger bandgap than GaAs [4, 32, 80]. In some cases, a combination of AlGaAs and InGaP window layers has also been used for achievement of efficiencies exceeding 27% [31]. Moreover, AlGaAs alloys have an intrinsic advantage in terms of high mobility, and that is why it has been most widely used for window application in GaAs solar cells, so far [81]. Similar to carrier selective layer, these window layers are heavily n- or p-type doped to the order of $10^{18}$ $cm^{-3}$ to achieve selectivity toward either electrons or holes, respectively. Unlike GaAs, lattice-matched, wide bandgap window layer for InP solar cell applications is not very well developed. Nevertheless, 22.1% and 24.2% efficient InP solar cells have respectively been achieved utilizing InGaAs and InAlAs as both a passivation and window layers [82-84]. Other III-V alloys which have been proposed as window layers for InP include GaAsSb, AlAsSb, AlGaAsSb, AlInAs, AlInAsSb, AlGaInAsSb, GaPSb, AlPSb, and

AlGaPSb [83]. Wanlass et al. have shown all of these alloys form significant positive conduction band offsets with InP, leading to a type-II band alignment and can be heavily doped to achieve electron confinement [83].

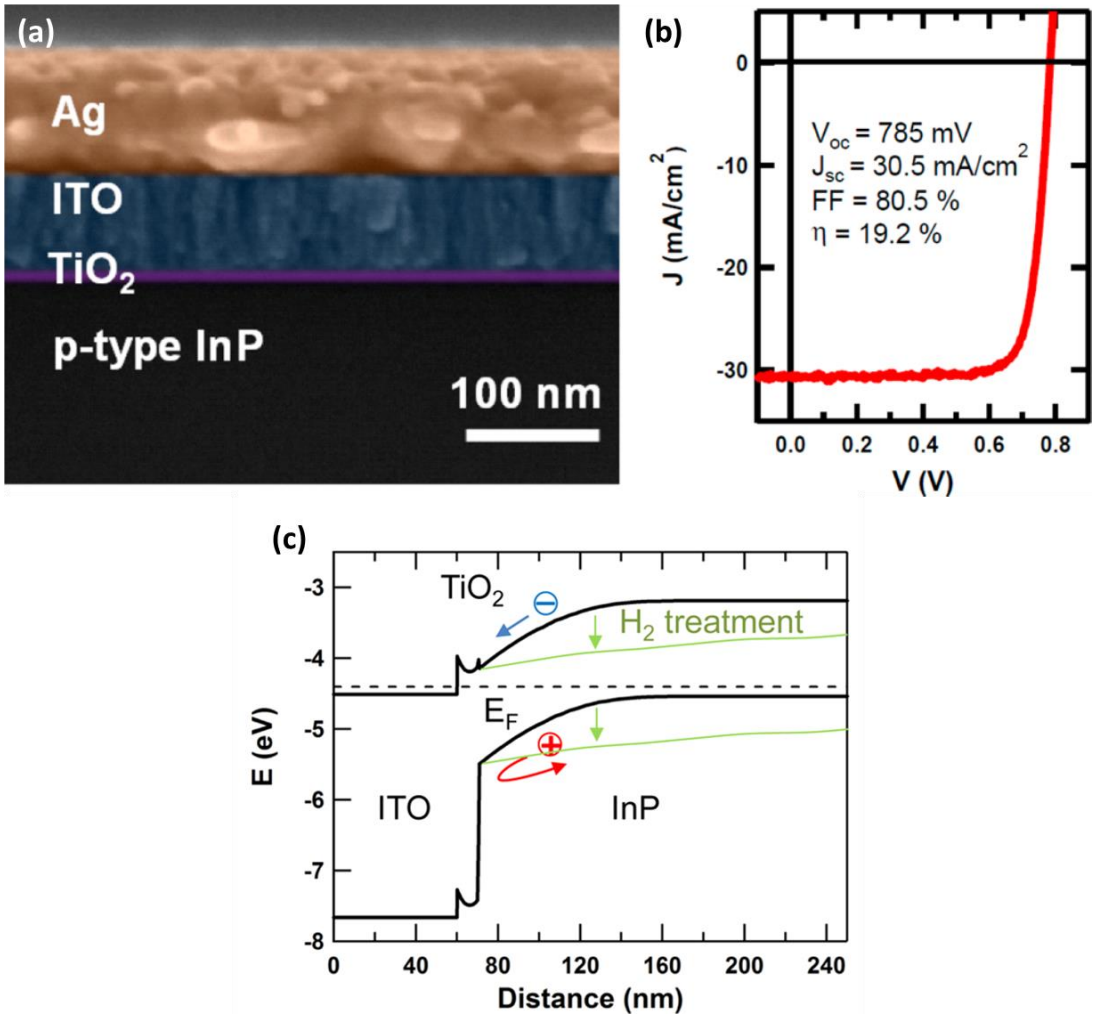


**Figure 1.** (a) SEM image of an InP solar cell using $TiO_2$ as an electron selective contact. (b) Corresponding IV curve for the solar cell shown in the left. (c) Schematic band diagram of the solar cell shows $TiO_2$ forms a type-I band alignment with InP with a small conduction band offset and a large valence band offset. After hydrogen plasma treatment the conduction band offset is further reduced for electron transport. *[Figure 1 has been reprinted (adapted) with permission from ref [92] Copyright © 2014 American Chemical Society]*

## 4. Electron Selective Contacts

In general, electron selective contacts are heavily n-type doped wide bandgap materials with low work function [75, 76, 85]. Until the last few years, carrier selectivity and carrier selective layers were not commonly used terminology, and researchers used the term heterojunction for almost all kinds of junctions between two different materials. However, in many cases, the rationale behind the concept of using these heterojunctions for solar cells application was very similar to that of carrier selective layers [86]. One of the best examples is the widely reported high-efficiency ITO/p-InP heterojunction solar cell. During the 90's ITO junction with InP was very popular for achieving very high efficiencies [87-89]. At that time, it was postulated that such high efficiency was due to the formation of buried homojunction between ITO and InP [87]. However, we have recently shown that the high efficiency of ITO/InP arises because of the combined effect of passivation and electron selectivity [86]. Passivation is a result of the formation of In(PO)x bond at the ITO/InP interface [90], whereas the carrier selectivity is due to heavy doping of ITO. In this section, we review some of the recent results on non-epitaxial electron selective contacts used for III-V solar cells.

### 4.1 Metal Oxides

In recent times, wide band gap transition metal oxides have gained massive popularity for application as carrier selective contacts, mainly because they can be heavily doped at low temperatures and are stable in ambient conditions. Several oxides such as $TiO_2$ [91], ZnO [86, 92-94], and $Ta_2O_5$ [95] have given promising results for InP solar cells. Figure 1 (a) shows a cross-sectional SEM image of an InP solar cell using $TiO_2$ as an electron selective contact (ESC). Using $TiO_2$ as electron selective contact, Yin et al. were able to achieve an efficiency of ~19.2% with a $V_{oc}$ and $J_{sc}$ of 785 mV and $J_{sc}$ of 30.5 mA/cm$^2$ [91]. They show that to achieve high efficiency,

$TiO_2$ needs to be in an amorphous phase and an additional step of hydrogen plasma treatment is required to passivate the shallow zinc acceptors in p-type InP. Neutralization of the shallow zinc acceptors enhanced the effective minority carrier lifetime. In a similar work, we have shown that the use of an i-InP over p-InP significantly can eliminate the reuqirement of hydrogen plasma treatement and also reduces the complexity of hydrogen plasma treatment, which may lead to the formation of In-droplet on the surface of InP [86]. Also, the removal of the plasma treatment step overwhelmingly improved the reproducibility of these heterojunction solar cells. Reddy et al. obtained similar results and showed that high-efficiency InP-based solar cell can be obtained using amorphous $Ta_2O_5$. For both ZnO and $Ta_2O_5$ ESCs, high open circuit voltage was obtained, with a maximum $V_{oc}$ of 822 and 815 mV, respectively [86, 95].

Furthermore, for both $Ta_2O_5$ [95] and ZnO [86], there was a significant improvement in the minority carrier lifetime, which shows that both $Ta_2O_5$ and ZnO can act as passivation layers as well as electron selective contact. Reddy et al. performed a series of photoluminescence (PL) measurements to show that solar cells with $Ta_2O_5$ (see figure 2(a) and 2(d)) show brighter PL compared to ITO/InP solar cells (see Figure 2(a) and 2(c)), signifying better passivation. Passivation due to $Ta_2O_5$ is also reflected in the lifetime measurement shown in Figure 2(b). We recently demonstrated that the passivation of InP in the presence of oxide is due to oxidation of phosphorus-rich InP surface, which leads to the formation of $InPO_x$ bond at the oxide/InP interface [86].

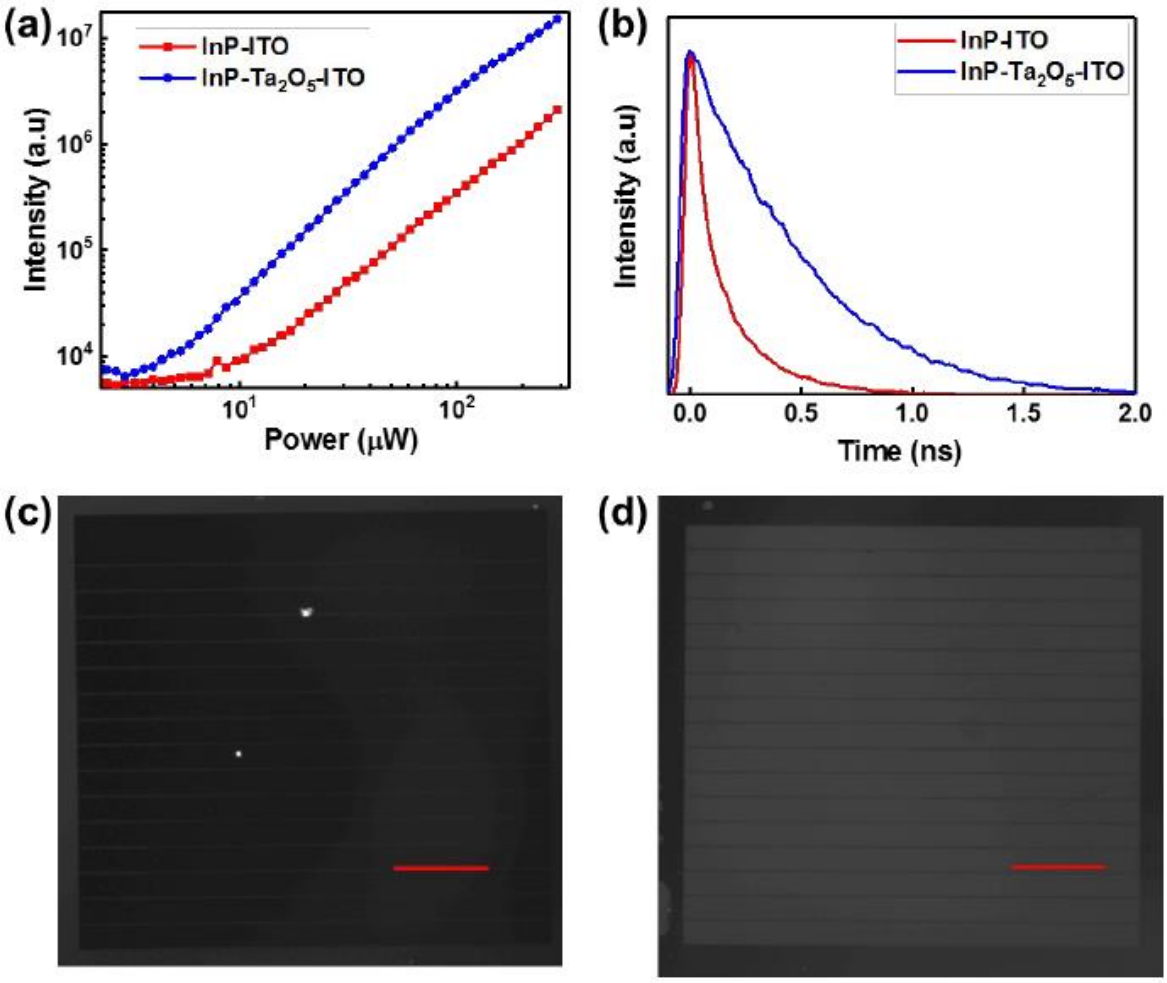


**Figure 2.** (a) PL intensity vs. excitation power profile showing that radiative recombination in ITO/InP solar cells is higher than ITO/$Ta_2O_5$/InP solar cells. (b) Comparative TRPL results showing significant improvement in the lifetime for ITO/$Ta_2O_5$/InP solar cells in comparison to ITO/InP solar cell. (c) and (d) shows the PL mapping on ITO/InP solar cells and ITO/$Ta_2O_5$/InP solar cell, respectively (the scale bar is 2 mm) *[Figure 2 has been reprinted (adapted) with permission from ref [96]. Copyright © 2019 The Royal Society of Chemistry]*

Another essential aspect of an ESC is its application to nanowire solar cells, where doping and window layer growth can be even more complicated than planar film growth [96-98]. We recently proposed a radial junction nanowire device structure that usage electron selective contact for charge carrier separation, thereby eliminating the requirement of the conventional p-n junction, and significantly reducing complexities associated with the growth and doping of III-V nanowires [99]. Figure 3(a) shows a 2-D schematic of the proposed InP solar cell. We showed that the use of an electron selective contact not only improved its electronic behavior but also improved the optical response of the nanowire solar cell [100]. Improved optical response of InP solar cells in the presence of an oxide-based carrier selective contact is a result of reduced electric field screening as well as optical mode confinement (see Figure 3(c)) [99]. We have shown that the $J_{sc}$ can improve by as much as 7 $mA/cm^2$ for an optimized thickness of the oxide layer (see Figure 3(b)). Furthermore, an oxide-based selective contact can generate a built-in electric field of the order of $10^8$ V/m, when the InP core is heavily doped to the order of $10^{18}$ $/cm^3$ [99, 101]. Such high electric field makes it possible to achieve very high efficiency even when material lifetime (diffusion length) is extremely poor [99]. In a separate paper, we experimentally verified that the

enhanced absorption and charge carrier separation in a nanowire solar cell in the presence of an optimized oxide based electron selective contact [100].

**Figure 3.** (a) 2-D schematic of the proposed InP solar cell using carrier selective contact. (b) FDTD simulation showing that with an optimized thickness of oxide layer $J_{sc\ (ideal)}$ can be improved by as much as 7 mA/cm$^2$. (c) Absoptance vs. wavelength curve shows enhanced absorption in oxide coated InP compared to bare InP. *[Figure 3(a)-(c) has been reprinted (adapted) with permission from ref [100]. Copyright © 2019 IEEE]*

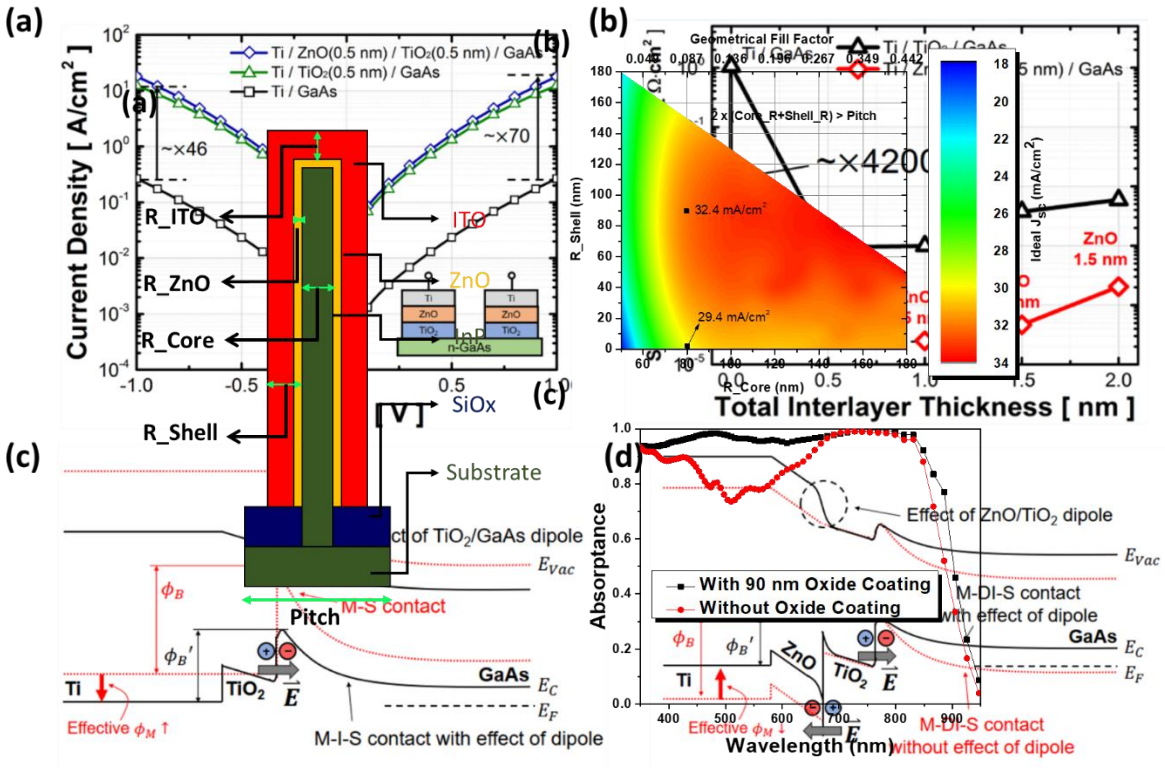

**Figure 4.** (a) J-V characteristics corresponding to Ti/GaAs, Ti/$TiO_2$/GaAs and Ti/ZnO/$TiO_2$/GaAs contact structures. (a) Contact resistivity of Ti/$TiO_2$/GaAs MIS contacts, with and without different thickness of ZnO interlayer. Band structure of (c) Ti/$TiO_2$/GaAs and (c) Ti/ $TiO_2$/$TiO_2$/GaAs showing the effect of an interlayer at the GaAs surface. *[Figure 4(a)-(d) has been reprinted (adapted) with permission from ref [104]. Copyright © 2016 American Chemical Society]*

Unlike InP, there are few reports on high-efficiency GaAs solar cells using metal oxide ESCs. Some of the oxides mentioned above, such as ZnO[102] have been tested as an ESC for GaAs but with little or no success. Nonetheless, there are several reports on the use of oxides for achieving low contact resistance for application in III-V transistors, which can also be implemented for solar cells application [103-106]. For examples, Kim et al. have shown that specific contact resistivity of $9.38 \times 10^{-4}$ $\Omega \cdot cm^2$ can be achieved for Ti/$TiO_2$(0.5 nm)/n-GaAs diode structure, and a further improvement in contact resistivity was demonstrated in the presence of an additional layer of ZnO [103]. For Ti/ZnO(0.5 nm)/$TiO_2$(0.5 nm)/n-GaAs diode structure the specific contact resistivity was reduced to as low as $2.51 \times 10^{-5}$ $\Omega \cdot cm^2$. Figures 4(a) and 4(b) show the improvement in J-V characteristics and contact resistivity of Ti/GaAs contact after the deposition of $TiO_2$ and ZnO/$TiO_2$ interlayers. Corresponding band diagrams of Ti/$TiO_2$/GaAs and Ti/$TiO_2$/ZnO/GaAs diodes are respectively shown in Figure 4(c) and 4(d). The band diagram shows that the use of ZnO interlayer in between $TiO_2$ and GaAs induces a dipole that is opposite to the dipole induced at the $TiO_2$/GaAs interface, leading to a reduced effective work function, which in turn results in low contact resistance. In addition to $TiO_2$ and ZnO, other oxides such as $HfO_2$, $Al_2O_3$, and $ZrO_2$ have readily been used to achieve very low specific contact resistivity for GaAs [103, 104, 106]. Often, bilayer of oxides (such as $TiO_2$/$Al_2O_3$, $TiO_2$/$HfO_2$, etc.) has been found to be more suitable for achieving low contact resistance in comparison to single layer of oxides [103, 104]. Several of

these oxides can also passivate GaAs [46, 59, 62] while ensuring low contact resistivity and proper band alignment, therefore, in the near future, one of these oxides may act as an efficient ESC for GaAs solar cells.

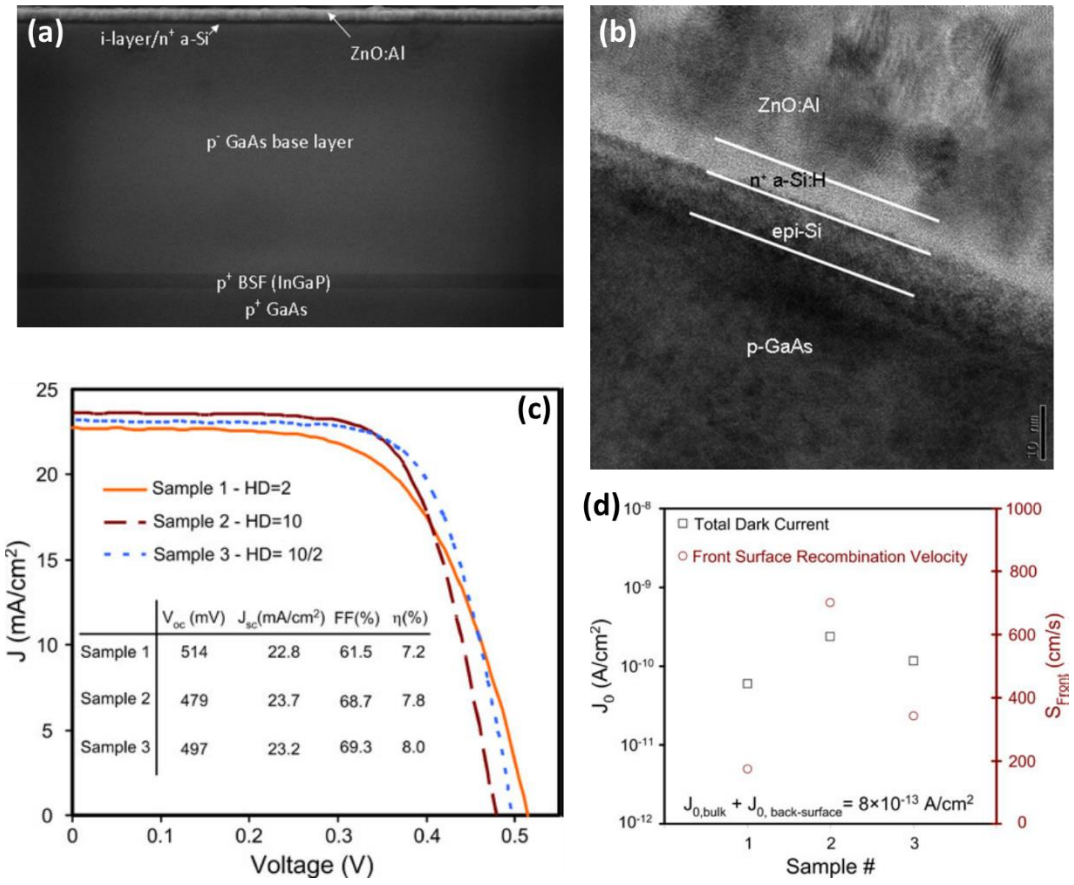


**Figure 5.** (a) FESEM image of a GaAs solar cell utilizing $n^+$ a-Si as an electron selective contact. (b) High resolution cross-sectional TEM image showing successful deposition of a-Si on GaAs at 200 $^oC$. (c) J-V characteristics corresponding to three different kind of samples. (d) Dark current density and front surface recombination velocity for three different kind of samples. *[Figure 5(a)-(d) has been reprinted (adapted) with permission from ref [117]. Copyright © 2011 IEEE]*

### 4.2 Other Inorganic Materials

Other than metal oxides, some sulfide materials such as CdS [107-110], ZnS [111] and $MoS_2$ [112-114] have been used to make a heterojunction solar cell with InP and GaAs. Advantage of using sulfides is that they can provide very high-quality passivation for both InP and GaAs to achieve

surface defect densities as low as $10^{10} – 10^{11}$ $cm^{-2}eV^{-1}$ [41, 49, 58] . Saito et al. demonstrated CdS/InP heterojunction solar cells achieving efficiencies higher than 17% [115]. They used a p-type InP and deposited a CdS layer of thickness 40-100 nm along with a transparent conducting oxide (TCO) based on ZnO and ITO, to form the heterojunction. They find that ITO/CdS/InP solar cells work better than ZnO/CdS/InP solar cells because ITO/CdS/InP solar cells form a lower contact resistance as compared to ZnO/CdS/InP solar cells. Also, thinner CdS layers gave higher efficiency compared to thicker CdS layers. It is now well known that with an increase in the thickness of ESC the bulk defect density of ESC may deteriorate the overall efficiency of the solar cell [86].

In a more recent work on sulfide-based selective contact for InP, Lin et al. have shown that 2-D $MoS_2$ layer forms type-I band alignment with InP and the heterostructure can be electrically tuned by application of an external voltage to achieve an efficient charge carrier separation and collection [112]. By varying the voltage from 0 to +6V, they were able to optimize the efficiency of $MoS_2$/InP solar cell from 4% to 7% [112]. They show that the change in photovoltaic behavior with the application of an external gate voltage is a direct result of reduced conduction band offset of $MoS_2$ with InP. Another sulfide which has widely been used to form a heterojunction with InP is ZnS. In particular, very promising results have been obtained for InP quantum dots passivated with a ZnS outer layer [111].

Furthermore, researchers have successfully utilized an a-Si:H layer as ESC for GaAs solar cells [116]. Shahrjerdi et al. show that GaAs solar cells with an efficiency of ~8% can be fabricated utilizing a-Si:H as an electron selective contact. The device (shown in Figure 5(a) and 5(b)) utilizes a combination of i-a-Si-H and $n^+$ a-Si-H layers, respectively for passivation and carrier selectivity. Moreover, they found that the hydrogen dilution layer in a-Si:H significantly influenced the efficiency of these cells. The hydrogen dilution level in the above case is defined as the ratio of $H_2$

gas flow to $SiH_4$ gas flow. Figure 5(c) shows J-V characteristics corresponding to three different kinds of solar cells fabricated with different hydrogen dilution levels in a-Si. According to authors, the best result was obtained for maximum hydrogen dilution level of 10. Also, the complete device was fabricated at a temperature lower than 200 $^oC$, which can reduce the thermal budget of the fabrication processes. Moreover, a-Si:H also provided good enough passivation for GaAs with a surface recombination velocity as low as 200 cm/s (see Figure 5(d)) [116]. A detailed interface analysis showed that the passivation of GaAs with a-Si:H is a combined result of dangling bond passivation due to hydrogen content in the a-Si:H as well as field-effect passivation due to a small conduction band and a large valence band offset with GaAs [116].

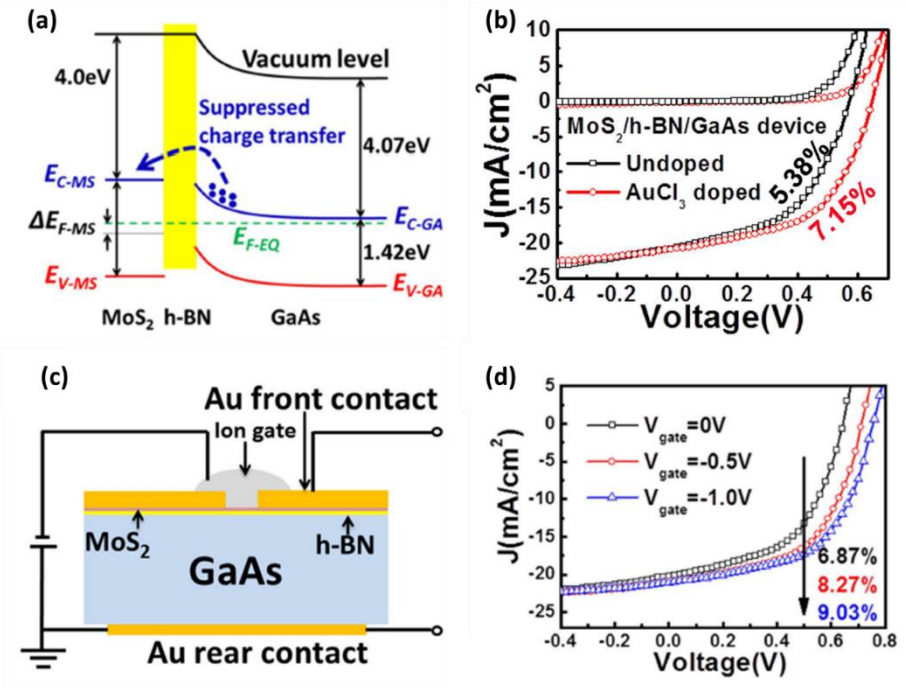

**Figure 6.** (a) Band diagram of $MoS_2$/h-BN/GaAs solar cells. (b) J-V curve of $MoS_2$/h-BN/GaAs solar cell with and without doping. (c) 2-D schematic of the heterojunction solar cell under ion gate bias. (d) Effect of biasing on the J-V curve of the heterojunction solar cell. *[Figure 6(a)-(d) has been reproduced from reference [118] under Creative Commons Attribution 4.0 International License.]*

In another work, Lin et al. have shown the fabrication of an efficient GaAs solar cell utilizing 2-D $MoS_2$. 2-D materials are particularly interesting because their Fermi level can be tuned fairly easily through chemical doping or gate biasing [117-120]. In this work, authors use both chemical doping as well as gate biasing to tune the $MoS_2$ Fermi level to achieve the maximum potential of the device. They were able to improve the efficiency of $MoS_2$/GaAs solar cell from 5.92% to 9.03% utilizing a h-BN passivation layer and a gate bias [117]. Figure 6(a) shows the band alignment of undoped $MoS_2$ with n-type GaAs in presence of h-BN monolayers, whereas, Figure 6(b) shows that after doping of $MoS_2$ with $AuCl_3$ the $V_{oc}$ of $MoS_2$/h-BN/GaAs heterojunction solar cell improved from 0.56 V to 0.64 V. Further improvement in the heterojunction solar cell was achieved through electrical gating. A 2-D schematic of device structure used for electrical gating of the solar cell is shown in Figure 6(c). It is quite apparent from the J-V curve shown in Figure 6(d) that there was improvement in solar cell performance under gate biasing. In particular, the $V_{oc}$ of the solar cell improved from 0.64 V to 0.72 V to 0.76 V under a bias of 0V, -0.5 V and -1.0 V, respectively.

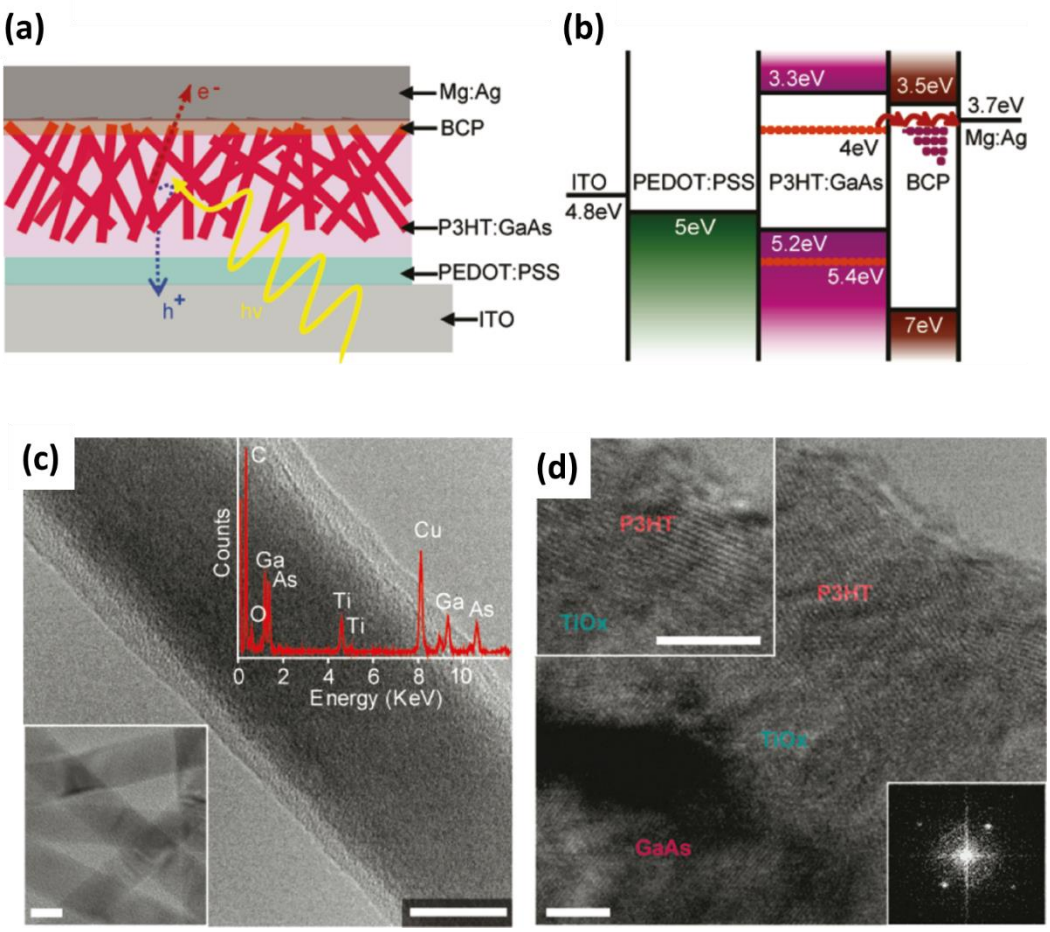


**Figure 7.** (a) 2-D schematic of GaAs hybrid nanowire solar cell. (b) Band alignment of GaAs with the organic materials used in (a). (c) Cross sectional bright filed TEM image of the heterojunction solar cell after $TiO_x$ deposition. $TiO_x$ is further confirmed by EDS measurement. (d) HRTEM image of a P3HT lamellar structure over $TiO_2$. *[Figure 7 has been reprinted (adapted) with permission from ref [125]. Copyright © 2011 American Chemical Society]*

### 4.3 Organic Materials

In addition to inorganic carrier selective materials, some organic materials have also been investigated for the fabrication of organic/Inorganic heterojunction solar cells [121-123]. A solar cell consisting of a combination of organic and inorganic material is known as a hybrid solar cell. So far, the reported efficiencies of these hybrid solar cells remain considerably low compared to some of the best reported III-V solar cells based on inorganic electron selective contact. However, the simplicity and low cost of organic materials make hybrid solar cells a vital contender for future applications. In particular, organic material provides an easy and cost-effective means to form selective contacts for nanowire solar cells. An example of a hybrid GaAs nanowire solar cell is shown in Figure 7(a) [124]. To fabricate this solar cell, the nanowires grown using MOCVD were broken from the substrate to form a nanowire 'powder'. Subsequent fabrication of hybrid solar cell utilized the nanowire 'powder'. The complete nanowire solar cell fabrication process was solution based and was performed at low temperatures. The solar cell structure consisted of GaAs nanowires embedded in P3HT, ITO/PEDOT:PSS as hole selective contact and BCP as electron selective contact. Figure 7(b) shows the band alignment of different organic materials with the GaAs nanowire embedded in P3HT. In the same paper [124], authors also study the effect of $TiO_x$ passivation (see Figure 7(c) and 7(d)) on the hybrid solar cell. Authors show that in presence of a $TiO_x$ passivation layer, $J_{sc}$ of the hybrid solar cell improved by almost 20% compared to unpassivated hybrid nanowire solar cell. However, even under optimized conditions, the authors were able to achieve only 2.36% photo conversion efficiency. Other organic materials that have been used as an ESC for III-V solar cells include bathocuproine (BCP) [124], PTCDA, poly(3-hexylthiophene) [122], $C_{60}$ and its derivatives [121, 123].

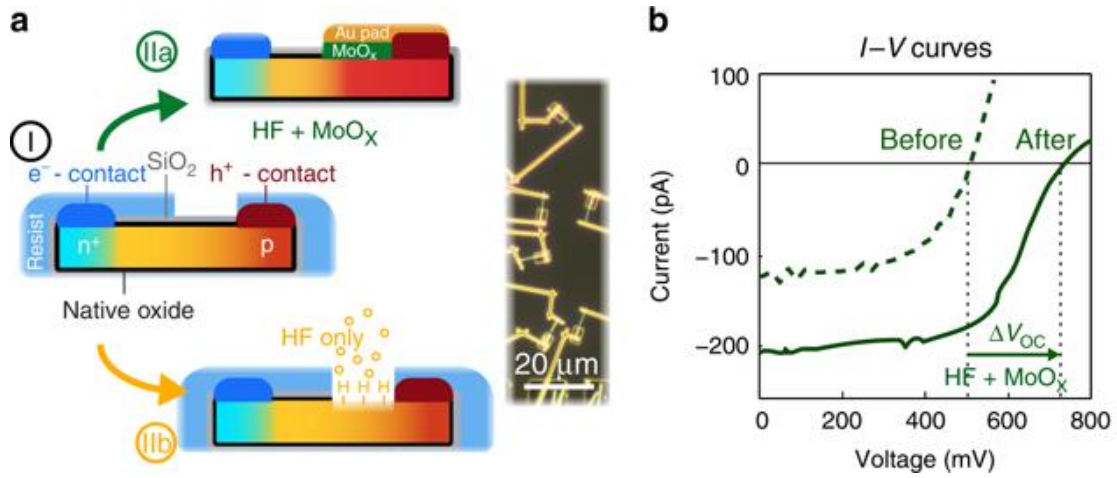


**Figure 8.** (a) Schematic showing the fabrication of single nanowire solar cell using $MoO_x$ as the carrier selective contact. (I) shows the nanowire with metal contacts on n- and p-side of the device, (IIa) shows removal of e-beam resist to deposit $MoO_x$ on the p-side, (IIb) shows HF treatment of nanowire before the deposition of MoOx. Also shown is an optical microscope image of single nanowire solar cells with MoOx contacts. (b) IV curve of the single nanowire solar cell before and and after HF treatment followed by $MoO_x$ deposition. *[Figure 8 has been reproduced from reference [128] under Creative Commons License.]*

## 5. Hole Selective Contacts

Unlike ESCs, there are very few reports on HSCs for III-V solar cells. In the next few sections, we review a few of these hole selective contacts.

### 5.1 Oxides and other Inorganic Materials

Molybdenum oxide ($MoO_x$) has been very successful as a hole selective material for silicon solar cells mainly because of their large work function which can be tuned between 5.75-6.70 eV by changing the deposition conditions [125, 126]. However, so far, there is no report of using $MoO_x$ as a hole selective contact for planar III-V solar cells. Nonetheless, very recently, Öner et al. have shown that $MoO_x$ can be used as a hole selective contact for InP nanowire solar cells [127]. They

show that an $MoO_x$ layer over p-InP nanowire leads to accumulation of holes at the MoOx/p-InP interface, leading to higher selectivity toward holes. The schematic of the fabrication of a single nanowire solar cell with hole selective contact is shown in Figure 8(a). The IV curves before and after $MoO_x$ deposition on the p-side of the p-i-n junction nanowire are shown in Figure 8(b). It is quite evident that $V_{oc}$ of the solar cell is increased from 500 to 730 mV in the presence of $MoO_x$. They also found that it is extremely desirable to treat the nanowire with HF before the deposition of $MoO_x$ layer. Previously, Pluchery et al. have shown the passivating behavior of HF for InP nanowires [128]. This indeed confirms that for high efficiency solar cells both passivation and carrier selectivity are equally important. The authors further substantiate the claim of increased hole selectivity for InP nanowire solar cell in presence of $MoO_x$, by designing three separate sets of devices. In the first set of devices, the $MoO_x$ was deposited on only the p-side of a p-i-n junction nanowire, in the second set, MoOx was deposited on only the n-side of a p-i-n junction nanowire and in the third set, MoOx was deposited on a completely p-doped InP nanowire. It was found that efficiency of the p-i-n InP nanowire solar cell only increased when $MoO_x$ is deposited on p-side of the solar cell, whereas the efficiency decreased substantially when $MoO_x$ was deposited on the n-side. Furthermore, deposition of $MoO_x$ on completely p-type nanowire resulted in a significant increase in the conductivity, thereby confirming the holes selectivity of $MoO_x$.

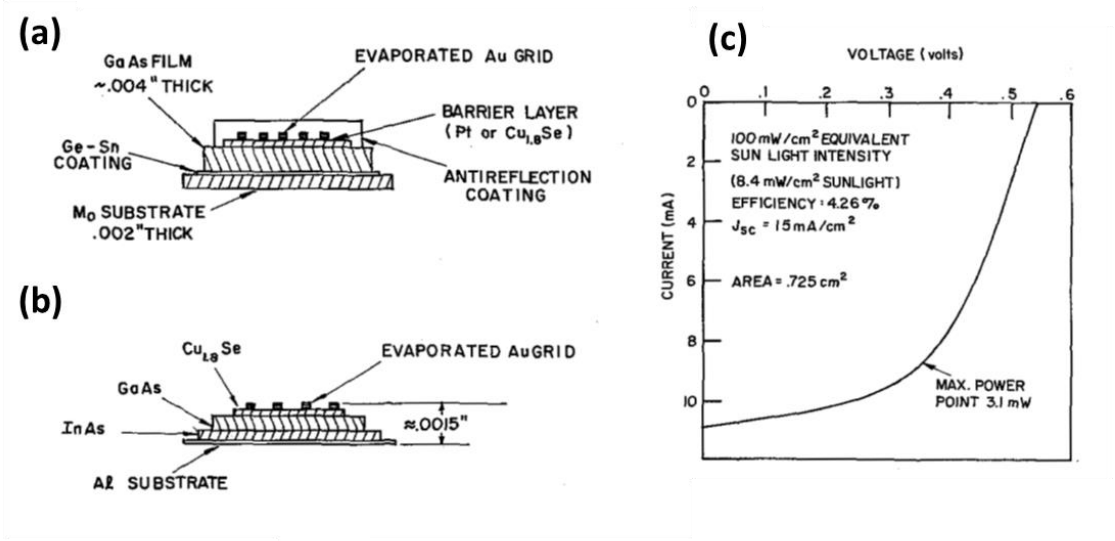


**Figure 9.** Polycrystalline GaAs solar cells grown on (a) molybdenum and (b) aluminium substrates, respectively. (c) IV corresponding to the most efficient solar cell obtained for $Cu_{1.8}$-Se/GaAs solar cell. *[Figure 9(a)-(c) has been reprinted (adapted) with permission from ref [132]. Copyright © 1967 IEEE]*

Even for GaAs, there very few reports on HSC. However, there have been few reports on p-type materials which make high-efficiency heterojunction solar cell with GaAs. For example, copper iodide (CuI) has been used to create a heterojunction with polycrystalline n-GaAs to achieve a $V_{oc}$ of 820 mV and $J_{sc}$ of 20 mA/cm$^2$ [129]. The efficiency of the device was not mentioned, but the values of $V_{oc}$ and $J_{sc}$ achieved are remarkable considering the GaAs was polycrystalline in nature with a thickness of ~100 μm and the complete fabrication of device was performed at a temperature less than 100 $^oC$. In addition, the CuI was very thick with thickness ranging from 2-3 μm [129]. Authors mention that to achieve optimum performance the n-type doping of GaAs

should be $10^{16}$ – $10^{17}$ $cm^{-3}$ and the CuI should be heavily doped [129]. However, they did not explicitly propose the reasons for such high performance of the solar cell. Nonetheless, recent results on CuI shows that it can be very easily p-type doped at room temperature with a hole concentration exceeding $10^{20}$ $cm^{-3}$ and has a work function of 5.6 eV which aligns very well with the valence band of GaAs [130]. A proper band alignment along with heavy p-type doping of CuI can be a reason for high efficiency of p-CuI/n-GaAs heterojunction solar cells.

Other p-type inorganic materials, which have been investigated but with little success for heterojunction with GaAs, include $Cu_2Se$ [131, 132], $Cu_2S$ [132] and CdTe [132]. Especially, from 1970-1990 there was a significant amount of work performed to achieve high efficiency using polycrystalline GaAs [130]. For example, Figure 9(a) and 9(b) shows two different kinds of solar cells based on polycrystalline GaAs grown on molybdenum (Mo) and aluminum (Al) substrates, respectively. Both of the cells used n-GaAs and a p-type $Cu_{1.8}Se$ to form the heterojunction [131]. However, for GaAs grown on Al, the back contact was InAs, whereas the back contact for GaAs grown on Mo was Ge-Sn [131]. The thickness of GaAs ranged from 50-200 μm. The IV corresponding to the most efficient device fabricated on Al-foil is shown in Figure 9(c). For AM1.5, researchers were able to achieve an efficiency of ~4.26% efficiency (on Al foil) with a $J_{sc}$ of 15 $mA/cm^2$, while achieving an efficiency of 4.6% for $Cu_{1.8}Se$-GaAs solar cells grown on molybdenum substrates [131]. Furthermore, researchers conclude that GaAs heterojunction solar cells grown both on the Al- and Mo- substrates were limited due to series, sheet and shunt resistance, which is also evident in the IV curve shown in Figure 10 (c) [131]. Now that there is a better understanding of working of heterojunction as well as carrier selective contact solar cells, these device structures can be revived to achieve high efficiency with low cost III-V materials. Based on discussion above, some of the improvements that can be made to achieve high efficiency

in $Cu_{1.8}Se$/n-GaAs solar cells include, (a) reduction in the thickness of GaAs to few 100 nm, (b) introduction of an additional passivation layer on both top and bottom of the cell before making metallic contacts, and (c) using a heavily doped p-type $Cu_{1.8}Se$.

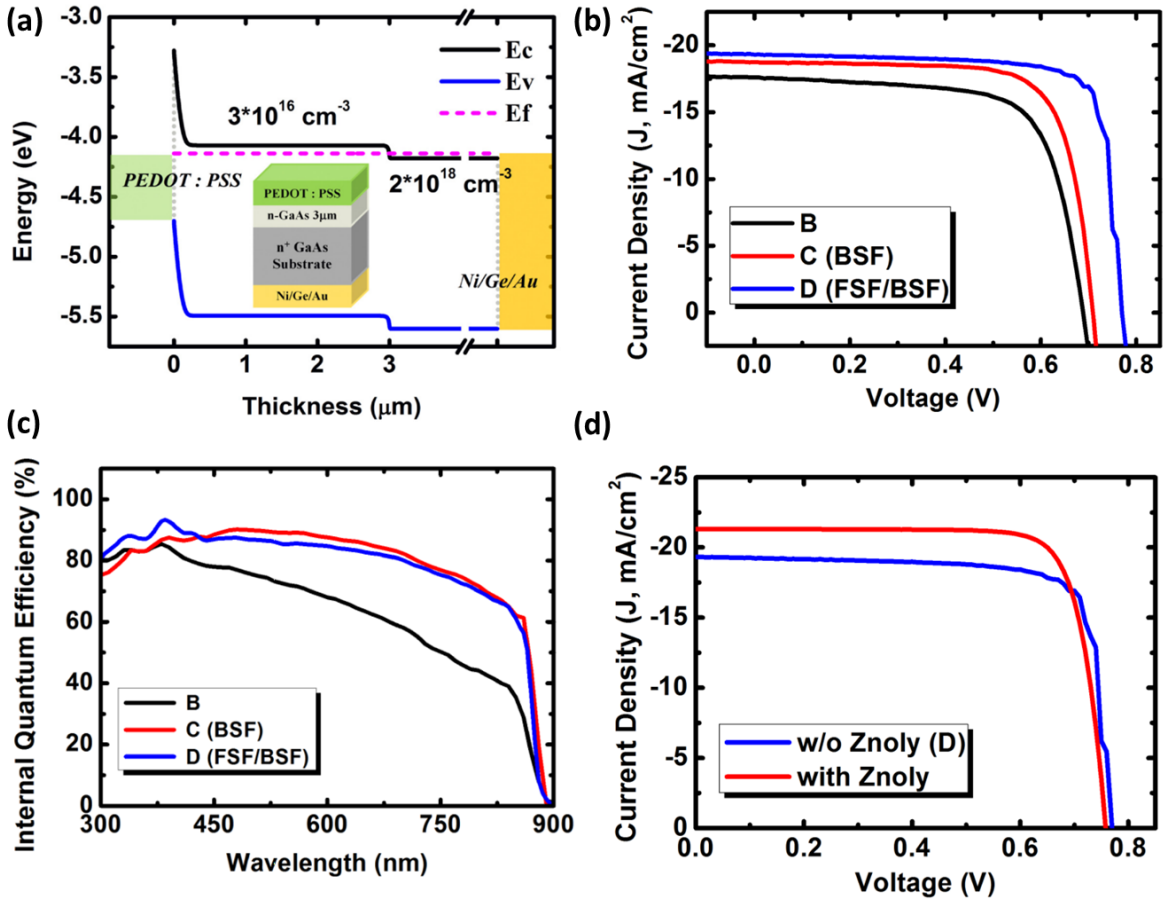


**Figure 10.** (a) Simulated band diagram for GaAs/PEDOT:PSS hybrid solar cell. Effect of front and back surface field on (b) IV and (c) external quantum efficiency of the hybrid solar cell. (d) Effect on the IV of the hybrid solar cell after addition of Zonyl in PEDOT:PSS. *[Figure 10(a)-(d) has been reprinted (adapted) with permission from ref [137]. Copyright © 1967 Optical Society of America]*

### 5.2 Organic Materials

Organic materials are low cost and can be deposited relatively easily; therefore, researchers have been trying to integrate III-Vs with them to reduce the overall cost of the solar cells. Most of these hybrid devices utilize p-type organic material and n-type GaAs to form the heterojunction. There is an abundance of reports on hybrid GaAs solar cells utilizing p-type organic material to form the junction. Some of these p-type organic materials which have shown exciting results include PEDOT:PSS and its derivatives [121, 122, 133-136], poly(3-hexylthiophene) [137], P3HT [137-140], and CuPc [141, 142]. Other than planar solar cells, organic material remains a popular choice for making a hybrid solar cell with nanowires [124, 137, 140, 143]. This is mainly because the organic solutions can be easily conformally coated over the nanowires. However, similar to ESC, even for HSC, the efficiency of hybrid solar cells remain relatively low compared to inorganic heterojunctions, because of low minority carrier lifetime, low carrier mobility, and high interface recombination [139, 140, 144].

A 2-D schematic and a band diagram of a n-GaAs based hybrid solar cell using PEDOT:PSS as a p-type contact is shown in Figure 10(a)[136]. Using the structure shown in Figure 10(a), Lin et al. were able to achieve an efficiency of 8.99%. They further reported that substantial improvement in IV characteristics (see Figure 10(b)) as well as quantum efficiency (see Figure 10(c)) can be realized in the proposed solar cell through the utilization of a front surface field (FSF) and back surface field (BSF) in the proposed hybrid solar cell [136]. It is quite evident from Figure 10 (b) and 10(c) that just by the implementation of a BSF layer, significant improvement in $J_{sc}$ can be realized. Moreover, after implementation of both BSF and FSF layer, the $V_{oc}$ of the hybrid device improved from 0.68 V to 0.77 V, the $J_{sc}$ improved from 17.51 mA/cm$^2$ to 19.31 mA/cm$^2$, and the efficiency improved from 9% to 11.86%, compared to hybrid solar cell without FSF/BSF layers.

Authors further improved the solar cell by treating PEDOT:PSS by MeOH and Zonly. After the addition of Znoly, the $J_{sc}$ of the hybrid solar cell improved from 19.31 mA/cm$^2$ to 21.3 mA/cm$^2$ (see Figure 10(d), leading to an improvement in efficiency from 11.86% to ~13% compared to without znoyl treated solar cell. Authors claimed that an increase in $J_{sc}$ after addition of Znoyl was a result of improved electrical conductivity and mobility of PEDOT:PSS layer after Znoyl treatment.

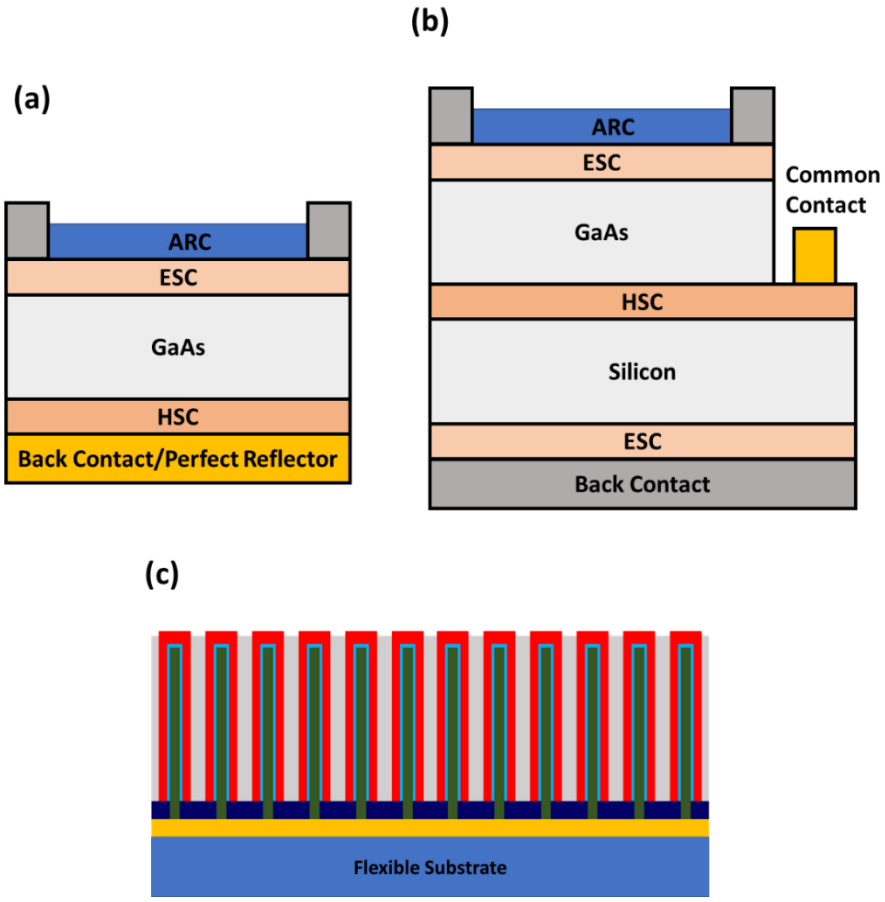


**Figure 11.** Three different device architectures using carrier selective contacts: (a) undoped planar III-V solar cell, (b) triple-junction tandem solar cell and (c) flexible nanowire solar cell. *[Figure 10(a) and (b) has been adapted with permission from ref [146]. Copyright © 2014 IEEE]*

## 6. Future prospects and new device concepts

III-V solar cells with carrier selective contacts hold enormous potential for future applications. For example, a detailed simulation of ITO/ZnO/i-InP/p-InP solar cell structure shows that under optimized conditions, these solar cells can achieve efficiencies comparable or better than that of homojunction p-i-n InP solar cells [86]. However, to achieve high efficiency, the interface defect density at ESC/InP should be less than $10^{13}$ $cm^{-2}eV^{-1}$. Such interface defect density has readily been achieved for different oxide/III-V interface [46], and therefore, III-V solar cells with high efficiencies can be achieved in the near future with proper optimization. Also, a more realistic approach toward achieving higher efficiencies might be the use of a separate passivation layer in conjunction with an ESC, for the separate function of passivation and electron selectivity, respectively.

Furthermore, carrier selective contact opens up the possibilities for the fabrication of new kind of device structures, some of which are shown in Figure 11. Figure 11(a) shows a device in which there is no requirement of doping and, charge carrier separation and collection happens only through selective contacts. The proposed device structure consists of an undoped III-V thin-film sandwiched between electron and hole selective contacts. It is expected that such a device will not only simplify the technical difficulties associated with the growth and doping of thin films but will also lead to higher efficiencies due to reduced optoelectronic loss [145, 146]. Furthermore, such devices have already realized for silicon, and it is a matter of time before it is implemented to III-Vs. Another kind of device which has recently been proposed by Islam et al. [145] is shown in Figure 11(b). The device is a simple version of a tandem solar cell. Their simulation results show that maximum efficiency of 39.3% can be achieved for this type of device. Realization of such a tandem cell can simplify several critical issues related to current tandem solar cells, such as current

matching, lattice-matched layer growth and stacking [147]. In Figure 11(c), a flexible nanowire array solar cell based on carrier selective contact is proposed. Because ESC based III-V solar cells can be fabricated at relatively low temperatures (less than 200 $^{o}$C), it is possible to integrate these cells to flexible plastic substrates [99, 101] and achieve low cost high efficiency flexible nanowire solar cells.

## 7. Conclusion

In this paper, different kinds of carrier selective contacts are reviewed for III-V solar cells application. It quite clear that carrier selective contacts hold enormous potential to overcome several of the technological challenges associated with doping and p-n junction formation. However, as it happens with any new technology, several challenges need addressing before these carrier selective contacts can be deployed for any commercially useful application. For example, the reported efficiencies for InP and GaAs solar cells based on the carrier selective contacts remain way below the highest reported efficiencies of GaAs and InP using standard p-i-n architecture [148]. Though there is no detailed study available, it seems that carrier selective contact based solar cells may be limited due to high interface defect density. Moreover, unlike silicon, research in III-V solar cells is relatively slow, and therefore, much more effort is required by the III-V research community to adopt, reproduce and improve on the work done on silicon solar cells with selective contacts to the III-V solar cells. In addition, a lot can also be learned from III-V MOSFETs, especially those related to passivation and low contact resistance fabrication, which can also be implemented for solar cell applications. Nonetheless, carrier selective contacts hold enormous potential for future applications, especially in cases where doping, controlled p-n junction formation, and the alloy composition control can be complicated for the fabrication of III-

V solar cells. Also, the use of carrier selective contacts for charge carrier separation allows for the fabrication of solar cell devices which would otherwise be more complicated.

**Acknowledgement**

The Australian Research Council is acknowledged for the financial support and the Australian National Fabrication Facility, ACT node is acknowledged for access to the facilities for some of the work referred to in this review.

**References:**

[1] C. Battaglia, A. Cuevas, S. De Wolf, High-efficiency crystalline silicon solar cells: status and perspectives, Energy Environ. Sci., 9 (2016) 1552-1576.https://doi.org/10.1039/C5EE03380B
[2] S. Mokkapati, C. Jagadish, III-V compound SC for optoelectronic devices, Materials Today, 12 (2009) 22-32.https://doi.org/10.1016/s1369-7021(09)70110-5
[3] V.M. Andreev, Application Of III–V Compounds In Solar Cells, in: J.M. Marshall, D. Dimova-Malinovska (Eds.) Photovoltaic and Photoactive Materials — Properties, Technology and Applications, Springer Netherlands, Dordrecht, 2002, pp. 131-156.
[4] B.M. Kayes, H. Nie, R. Twist, S.G. Spruytte, F. Reinhardt, I.C. Kizilyalli, G.S. Higashi, 27.6% Conversion efficiency, a new record for single-junction solar cells under 1 sun illumination, in: 2011 37th IEEE Photovoltaic Specialists Conference, 2011, pp. 000004-000008.
[5] O.D. Miller, E. Yablonovitch, S.R. Kurtz, Strong Internal and External Luminescence as Solar Cells Approach the Shockley–Queisser Limit, IEEE J. Photovolt., 2 (2012) 303-311.https://doi.org/10.1109/JPHOTOV.2012.2198434
[6] M.A. Green, Radiative efficiency of state-of-the-art photovoltaic cells, Progress in Photovoltaics: Research and Applications, 20 (2012) 472-476.https://doi.org/10.1002/pip.1147
[7] E. Yablonovitch, O.D. Miller, The opto-electronic physics which just broke the efficiency record in solar cells (presentation video), SPIE, 2014.
[8] K.-T. Shiu, J. Zimmerman, H. Wang, S.R. Forrest, Ultrathin film, high specific power InP solar cells on flexible plastic substrates, Appl. Phys. Lett., 95 (2009) 223503.https://doi.org/10.1063/1.3268805
[9] T.R. Kelsey A. W. Horowitz, Brittany Smith, and Aaron Ptak, A Techno-Economic Analysis and Cost Reduction Roadmap for III-V Solar Cells, in, National Renewable Energy Laboratory, Golden, Colarado, USA, 2018.
[10] J.S. Ward, T. Remo, K. Horowitz, M. Woodhouse, B. Sopori, K. VanSant, P. Basore, Techno-economic analysis of three different substrate removal and reuse strategies for III-V solar cells, Progress in Photovoltaics: Research and Applications, 24 (2016) 1284-1292.https://doi.org/10.1002/pip.2776
[11] A. Goodrich, M. Woodhouse, A Manufacturing Cost Analysis Relevant to Single- and Dual-Junction Photovoltaic Cells Fabricated with III-Vs and III-Vs Grown on Czochralski Silicon, in, National Renewable Energy Laboratory (NREL), Colarado, United States, 2013.

[12] M. Hettick, M. Zheng, Y. Lin, C.M. Sutter-Fella, J.W. Ager, A. Javey, Nonepitaxial Thin-Film InP for Scalable and Efficient Photocathodes, J. Phys. Chem. Lett., 6 (2015) 2177-2182.https://doi.org/10.1021/acs.jpclett.5b00744
[13] R. Kapadia, Z. Yu, M. Hettick, J. Xu, M.S. Zheng, C.-Y. Chen, A.D. Balan, D.C. Chrzan, A. Javey, Deterministic Nucleation of InP on Metal Foils with the Thin-Film Vapor–Liquid–Solid Growth Mode, Chem. Mater., 26 (2014) 1340-1344.https://doi.org/10.1021/cm403403v
[14] H.-P. Wang, C.M. Sutter-Fella, P. Lobaccaro, M. Hettick, M. Zheng, D.-H. Lien, D.W. Miller, C.W. Warren, E.T. Roe, M.C. Lonergan, H.L. Guthrey, N.M. Haegel, J.W. Ager, C. Carraro, R. Maboudian, J.-H. He, A. Javey, Increased Optoelectronic Quality and Uniformity of Hydrogenated p-InP Thin Films, Chem. Mater., 28 (2016) 4602-4607.https://doi.org/10.1021/acs.chemmater.6b01257
[15] C.J. Funch, A.L. Greenaway, J.W. Boucher, R. Weiss, A. Welsh, S. Aloni, S.W. Boettcher, Close-spaced vapor transport reactor for III-V growth using HCl as the transport agent, J. Cryst. Growth, 506 (2019) 147-155.https://doi.org/https://doi.org/10.1016/j.jcrysgro.2018.10.031
[16] A.J. Ritenour, R.C. Cramer, S. Levinrad, S.W. Boettcher, Efficient n-GaAs Photoelectrodes Grown by Close-Spaced Vapor Transport from a Solid Source, ACS Appl. Mater. Interfaces, 4 (2012) 69-73.https://doi.org/10.1021/am201631p
[17] J.W. Boucher, A.L. Greenaway, K.E. Egelhofer, S.W. Boettcher, Analysis of performance-limiting defects in pn junction GaAs solar cells grown by water-mediated close-spaced vapor transport epitaxy, Sol. Energy Mater. Sol. Cells, 159 (2017) 546-552.https://doi.org/https://doi.org/10.1016/j.solmat.2016.10.004
[18] E. Koskiahde, D. Cossement, R. Paynter, J.P. Dodelet, A. Jean, B.A. Lombos, Doping of GaAs epitaxial layers grown on (100) GaAs by close-spaced vapor transport, Can. J. Phys., 67 (1989) 251-258.https://doi.org/10.1139/p89-044
[19] M. Heurlin, M.H. Magnusson, D. Lindgren, M. Ek, L.R. Wallenberg, K. Deppert, L. Samuelson, Continuous gas-phase synthesis of nanowires with tunable properties, Nature, 492 (2012) 90.https://doi.org/10.1038/nature11652

https://www.nature.com/articles/nature11652#supplementary-information
[20] E. Barrigón, O. Hultin, D. Lindgren, F. Yadegari, M.H. Magnusson, L. Samuelson, L.I.M. Johansson, M.T. Björk, GaAs Nanowire pn-Junctions Produced by Low-Cost and High-Throughput Aerotaxy, Nano Lett., 18 (2018) 1088-1092.https://doi.org/10.1021/acs.nanolett.7b04609
[21] W. Metaferia, S. Sivakumar, A.R. Persson, I. Geijselaers, L.R. Wallenberg, K. Deppert, L. Samuelson, M.H. Magnusson, n-type doping and morphology of GaAs nanowires in Aerotaxy, Nanotechnology, 29 (2018) 285601.https://doi.org/10.1088/1361-6528/aabec0
[22] K. Tomioka, T. Tanaka, S. Hara, K. Hiruma, T. Fukui, III–V Nanowires on Si Substrate: Selective-Area Growth and Device Applications, IEEE J. Sel. Topics Quantum Electron., 17 (2011) 1112-1129.https://doi.org/10.1109/JSTQE.2010.2068280
[23] X.-Y. Bao, C. Soci, D. Susac, J. Bratvold, D.P.R. Aplin, W. Wei, C.-Y. Chen, S.A. Dayeh, K.L. Kavanagh, D. Wang, Heteroepitaxial Growth of Vertical GaAs Nanowires on Si (111) Substrates by Metal−Organic Chemical Vapor Deposition, Nano Lett., 8 (2008) 3755-3760.https://doi.org/10.1021/nl802062y
[24] T. Haggren, V. Khayrudinov, V. Dhaka, H. Jiang, A. Shah, M. Kim, H. Lipsanen, III–V nanowires on black silicon and low-temperature growth of self-catalyzed rectangular InAs NWs, Sci. Rep., 8 (2018) 6410.https://doi.org/10.1038/s41598-018-24665-9

[25] V. Dhaka, T. Haggren, H. Jussila, H. Jiang, E. Kauppinen, T. Huhtio, M. Sopanen, H. Lipsanen, High Quality GaAs Nanowires Grown on Glass Substrates, Nano Lett., 12 (2012) 1912-1918.https://doi.org/10.1021/nl204314z
[26] A.L. Greenaway, J.W. Boucher, S.Z. Oener, C.J. Funch, S.W. Boettcher, Low-Cost Approaches to III–V Semiconductor Growth for Photovoltaic Applications, ACS Energy Lett., 2 (2017) 2270-2282.https://doi.org/10.1021/acsenergylett.7b00633
[27] Y. Sun, X. Sun, S. Johnston, C.M. Sutter-Fella, M. Hettick, A. Javey, P. Bermel, Voc degradation in TF-VLS grown InP solar cells, in: 2016 IEEE 43rd Photovoltaic Specialists Conference (PVSC), 2016, pp. 1934-1937.
[28] U. Würfel, A. Cuevas, P. Würfel, Charge Carrier Separation in Solar Cells, IEEE J. Photovolt., 5 (2015) 461-469.https://doi.org/10.1109/JPHOTOV.2014.2363550
[29] K. Yoshikawa, H. Kawasaki, W. Yoshida, T. Irie, K. Konishi, K. Nakano, T. Uto, D. Adachi, M. Kanematsu, H. Uzu, K. Yamamoto, Silicon heterojunction solar cell with interdigitated back contacts for a photoconversion efficiency over 26%, Nature Energy, 2 (2017) 17032.https://doi.org/10.1038/nenergy.2017.32
[30] R. Kamada, T. Yagioka, S. Adachi, A. Handa, K.F. Tai, T. Kato, H. Sugimoto, New world record Cu(In, Ga)(Se, S)2thin film solar cell efficiency beyond 22%, in: 2016 IEEE 43rd Photovoltaic Specialists Conference (PVSC), 2016, pp. 1287-1291.
[31] W.S. Yang, J.H. Noh, N.J. Jeon, Y.C. Kim, S. Ryu, J. Seo, S.I. Seok, High-performance photovoltaic perovskite layers fabricated through intramolecular exchange, Science, 348 (2015) 1234.https://doi.org/10.1126/science.aaa9272
[32] S.-T. Hwang, S. Kim, H. Cheun, H. Lee, B. Lee, T. Hwang, S. Lee, W. Yoon, H.-M. Lee, B. Park, Bandgap grading and Al0.3Ga0.7As heterojunction emitter for highly efficient GaAs-based solar cells, Sol. Energy Mater. Sol. Cells, 155 (2016) 264-272.https://doi.org/https://doi.org/10.1016/j.solmat.2016.06.009
[33] S.W. Glunz, M. Bivour, C. Messmer, F. Feldmann, R. Müller, C. Reichel, A. Richter, F. Schindler, J. Benick, M. Hermle, Passivating and Carrier-selective Contacts - Basic Requirements and Implementation, in: 2017 IEEE 44th Photovoltaic Specialist Conference (PVSC), 2017, pp. 2064-2069.
[34] M. Taguchi, A. Yano, S. Tohoda, K. Matsuyama, Y. Nakamura, T. Nishiwaki, K. Fujita, E. Maruyama, 24.7% Record Efficiency HIT Solar Cell on Thin Silicon Wafer, IEEE J. Photovolt., 4 (2014) 96-99.https://doi.org/10.1109/JPHOTOV.2013.2282737
[35] A. Cuevas, Y. Wan, D. Yan, C. Samundsett, T. Allen, X. Zhang, J. Cui, J. Bullock, Carrier population control and surface passivation in solar cells, Sol. Energy Mater. Sol. Cells, 184 (2018) 38-47.https://doi.org/https://doi.org/10.1016/j.solmat.2018.04.026
[36] R. Brendel, R. Peibst, Contact Selectivity and Efficiency in Crystalline Silicon Photovoltaics, IEEE J. Photovolt., 6 (2016) 1413-1420.https://doi.org/10.1109/JPHOTOV.2016.2598267
[37] P. Würfel, Limitations on Energy Conversion in Solar Cells, Physics of Solar Cells, (2007) 137-153.https://doi.org/doi:10.1002/9783527618545.ch7

10.1002/9783527618545.ch7
[38] S.R. Kurtz, J.M. Olson, D.J. Friedman, J.F. Geisz, K.A. Bertness, A.E. Kibbler, Passivation of Interfaces in High-Efficiency Photovoltaic Devices, MRS Proceedings, 573 (1999) 95.https://doi.org/10.1557/PROC-573-95
[39] S. Smit, Passivating selective contacts for silicon photovoltaics : solar cells designed by physics, in, Technische Universiteit Eindhoven,, Eindhoven, Netherlands, 2016, pp. 210.

[40] J. Melskens, B.W.H.v.d. Loo, B. Macco, L.E. Black, S. Smit, W.M.M. Kessels, Passivating Contacts for Crystalline Silicon Solar Cells: From Concepts and Materials to Prospects, IEEE J. Photovolt., 8 (2018) 373-388.https://doi.org/10.1109/JPHOTOV.2018.2797106
[41] J.S. Herman, F.L. Terry, Hydrogen sulfide plasma passivation of gallium arsenide, Appl. Phys. Lett., 60 (1992) 716-717.https://doi.org/10.1063/1.106547
[42] T. Ogawa, G. Wang, K. Murase, K. Hori, J. Arokiaraj, T. Soga, T. Jimbo, M. Umeno, Phosphine-added hydrogen plasma passivation of GaAs solar cell on Si substrate, in: Conference Record of the Twenty-Eighth IEEE Photovoltaic Specialists Conference - 2000 (Cat. No.00CH37036), 2000, pp. 1308-1311.
[43] T. Soga, T. Jimbo, G. Wang, K. Ohtsuka, M. Umeno, Hydrogen plasma passivation of GaAs on Si substrates for solar cell fabrication, J. Appl. Phys., 87 (2000) 2285-2288.https://doi.org/10.1063/1.372174
[44] M.T. Sheldon, C.N. Eisler, H.A. Atwater, GaAs Passivation with Trioctylphosphine Sulfide for Enhanced Solar Cell Efficiency and Durability, Adv. Energy Mater., 2 (2012) 339-344.https://doi.org/10.1002/aenm.201100666
[45] J.M. Olson, R.K. Ahrenkiel, D.J. Dunlavy, B. Keyes, A.E. Kibbler, Ultralow recombination velocity at Ga0.5In0.5P/GaAs heterointerfaces, Appl. Phys. Lett., 55 (1989) 1208-1210.https://doi.org/10.1063/1.101656
[46] J. Robertson, Y. Guo, L. Lin, Defect state passivation at III-V oxide interfaces for complementary metal–oxide–semiconductor devices, J. Appl. Phys., 117 (2015) 112806.https://doi.org/10.1063/1.4913832
[47] M. Passlack, M. Hong, J.P. Mannaerts, J.R. Kwo, L.W. Tu, Recombination velocity at oxide–GaAs interfaces fabricated by in situ molecular beam epitaxy, Appl. Phys. Lett., 68 (1996) 3605-3607.https://doi.org/10.1063/1.116652
[48] M. Passlack, M. Hong, R.L. Opila, J.P. Mannaerts, J.R. Kwo, GaAs surface passivation using in-situ oxide deposition, Appl. Surf. Sci., 104-105 (1996) 441-447.https://doi.org/https://doi.org/10.1016/S0169-4332(96)00184-5
[49] S.R. Lunt, G.N. Ryba, P.G. Santangelo, N.S. Lewis, Chemical studies of the passivation of GaAs surface recombination using sulfides and thiols, J. Appl. Phys., 70 (1991) 7449-7467.https://doi.org/10.1063/1.349741
[50] A. Sher, Y.H. Tsuo, J.E. Chern, W.E. Miller, INTERFACE STATES IN GaAs/LaF3 CONFIGURATIONS, in: G. Lucovsky, S.T. Pantelides, F.L. Galeener (Eds.) The Physics of MOS Insulators, Pergamon, 1980, pp. 280-284.
[51] L.E. Black, A. Cavalli, M.A. Verheijen, J.E.M. Haverkort, E.P.A.M. Bakkers, W.M.M. Kessels, Effective Surface Passivation of InP Nanowires by Atomic-Layer-Deposited Al2O3 with POx Interlayer, Nano Lett., 17 (2017) 6287-6294.https://doi.org/10.1021/acs.nanolett.7b02972
[52] A.B.M.O. Islam, T. Tambo, C. Tatsuyama, Passivation of GaAs surface by GaS, Vacuum, 59 (2000) 894-899.https://doi.org/https://doi.org/10.1016/S0042-207X(00)00397-3
[53] Y. Dong, X.M. Ding, X.Y. Hou, Y. Li, X.B. Li, Sulfur passivation of GaAs metal-semiconductor field-effect transistor, Appl. Phys. Lett., 77 (2000) 3839-3841.https://doi.org/10.1063/1.1331642
[54] V. Dhaka, A. Perros, S. Naureen, N. Shahid, H. Jiang, J.-P. Kakko, T. Haggren, E. Kauppinen, A. Srinivasan, H. Lipsanen, Protective capping and surface passivation of III-V nanowires by atomic layer deposition, AIP Advances, 6 (2016) 015016.https://doi.org/10.1063/1.4941063

[55] M. Passlack, R. Droopad, G. Brammertz, Suitability Study of Oxide/Gallium Arsenide Interfaces for MOSFET Applications, IEEE Trans. Electron Devices, 57 (2010) 2944-2956.https://doi.org/10.1109/TED.2010.2065950
[56] L. Lin, J. Robertson, Defect states at III-V semiconductor oxide interfaces, Appl. Phys. Lett., 98 (2011) 082903.https://doi.org/10.1063/1.3556619
[57] L. Zhou, B. Bo, X. Yan, C. Wang, Y. Chi, X. Yang, Brief Review of Surface Passivation on III-V Semiconductor, Crystals, 8 (2018).https://doi.org/10.3390/cryst8050226
[58] C.N. Rodica V. Ghiţă, Costel Cotirlan, Constantin Logofatu, On the passivation of gaas surface by sulfide compounds, Dig. J. Nanomater. Bios., 8 (2013) 1335-1344
[59] H. Hasegawa, M. Akazawa, Surface passivation technology for III–V semiconductor nanoelectronics, Appl. Surf. Sci., 255 (2008) 628-632.https://doi.org/https://doi.org/10.1016/j.apsusc.2008.07.002
[60] A.M. Green, W.E. Spicer, Do we need a new methodology for GaAs passivation?, J. Vac. Sci. Technol., A, 11 (1993) 1061-1069.https://doi.org/10.1116/1.578442
[61] C.J. Spindt, W.E. Spicer, Sulfur passivation of GaAs surfaces: A model for reduced surface recombination without band flattening, Appl. Phys. Lett., 55 (1989) 1653-1655.https://doi.org/10.1063/1.102228
[62] H. Hasegawa, M. Akazawa, A. Domanowska, B. Adamowicz, Surface passivation of III–V semiconductors for future CMOS devices—Past research, present status and key issues for future, Appl. Surf. Sci., 256 (2010) 5698-5707.https://doi.org/https://doi.org/10.1016/j.apsusc.2010.03.091
[63] H. Hasegawa, M. Akazawa, Interface models and processing technologies for surface passivation and interface control in III–V semiconductor nanoelectronics, Appl. Surf. Sci., 254 (2008) 8005-8015.https://doi.org/https://doi.org/10.1016/j.apsusc.2008.03.051
[64] W. Tsai, N. Goel, S. Koveshnikov, P. Majhi, W. Wang, Challenges of integration of high-κ dielectric with III–V materials (Invited Paper), Microelectron. Eng., 86 (2009) 1540-1543.https://doi.org/https://doi.org/10.1016/j.mee.2009.03.117
[65] Y. Xuan, H. Lin, P.D. Ye, Simplified Surface Preparation for GaAs Passivation Using Atomic Layer-Deposited High-$\kappa$Dielectrics, IEEE Trans. Electron Devices, 54 (2007) 1811-1817.https://doi.org/10.1109/TED.2007.900678
[66] C.L. Hinkle, E.M. Vogel, P.D. Ye, R.M. Wallace, Interfacial chemistry of oxides on InxGa(1−x)As and implications for MOSFET applications, Curr. Opin. Solid State Mater. Sci., 15 (2011) 188-207.https://doi.org/https://doi.org/10.1016/j.cossms.2011.04.005
[67] C.N. Eisler, M.T. Sheldon, H.A. Atwater, Enhanced performance of small GaAs solar cells via edge and surface passivation with trioctylphosphine sulfide, in: 2012 38th IEEE Photovoltaic Specialists Conference, 2012, pp. 000937-000940.
[68] M.V. Lebedev, Sulfur Adsorption at GaAs: Role of the Adsorbate Solvation and Reactivity in Modification of Semiconductor Surface Electronic Structure, J. Phys. Chem. B, 105 (2001) 5427-5433.https://doi.org/10.1021/jp0035434
[69] K.S.A. Butcher, R.J. Egan, T.L. Tansley, D. Alexiev, Sulfur contamination of (100) GaAs resulting from sample preparation procedures and atmospheric exposure, J. Vac. Sci. Technol., B: Microelectron. Nanometer Struct.--Process., Meas., Phenom., 14 (1996) 152-158.https://doi.org/10.1116/1.589018
[70] M. Schvartzman, V. Sidorov, D. Ritter, Y. Paz, Surface passivation of (100) InP by organic thiols and polyimide as characterized by steady-state photoluminescence, Semiconductor Science and Technology, 16 (2001) L68-L71.https://doi.org/10.1088/0268-1242/16/10/103

[71] M. Schvartzman, V. Sidorov, D. Ritter, Y. Paz, Passivation of InP surfaces of electronic devices by organothiolated self-assembled monolayers, J. Vac. Sci. Technol., B: Microelectron. Nanometer Struct.--Process., Meas., Phenom., 21 (2003) 148-155.https://doi.org/10.1116/1.1532026
[72] C. Nyamhere, J.R. Botha, A. Venter, Electrical characterization of deep levels in n-type GaAs after hydrogen plasma treatment, Phys. B (Amsterdam, Neth.), 406 (2011) 2273-2276.https://doi.org/https://doi.org/10.1016/j.physb.2011.03.052
[73] N. Elgun, E.A. Davis, Structure and electronic properties of hydrogenated amorphous GaP, J. Non-Cryst. Solids, 330 (2003) 226-233.https://doi.org/https://doi.org/10.1016/S0022-3093(03)00531-3
[74] X. Hou, X. Chen, Z. Li, X. Ding, X. Wang, Passivation of GaAs surface by sulfur glow discharge, Appl. Phys. Lett., 69 (1996) 1429-1431.https://doi.org/10.1063/1.117604
[75] F. Feldmann, M. Simon, M. Bivour, C. Reichel, M. Hermle, S.W. Glunz, Carrier-selective contacts for Si solar cells, Appl. Phys. Lett., 104 (2014) 181105.https://doi.org/10.1063/1.4875904
[76] E.T. Roe, K.E. Egelhofer, M.C. Lonergan, Limits of Contact Selectivity/Recombination on the Open-Circuit Voltage of a Photovoltaic, ACS Applied Energy Materials, 1 (2018) 1037-1046.https://doi.org/10.1021/acsaem.7b00179
[77] P. Gao, Z. Yang, J. He, J. Yu, P. Liu, J. Zhu, Z. Ge, J. Ye, Dopant-Free and Carrier-Selective Heterocontacts for Silicon Solar Cells: Recent Advances and Perspectives, Adv. Sci., 5 (2018) 1700547.https://doi.org/10.1002/advs.201700547
[78] A. Spies, M. List, T. Sarkar, U. Würfel, On the Impact of Contact Selectivity and Charge Transport on the Open-Circuit Voltage of Organic Solar Cells, Adv. Energy Mater., 7 (2017) 1601750.https://doi.org/10.1002/aenm.201601750
[79] J.M. Mar, State-of-the-art of III-V Solar Cell Fabrication Technologies, Device Designs and Applications, in, 2004.
[80] D.M. James P. Connolly, III-V solar cells, in, Arxiv, 2013.
[81] M.R. M. Bivour, F. Feldmann, M. Hermle, S. Glunz, Requirements for Carrier Selective Silicon Heterojunctions, in: 24th Workshop on Crystalline Silicon Solar Cells & Modules: Materials and Processes, Colorado, United States 2014.
[82] Raj K. Jain, InP solar cell with WINDOW LAYER, in: U.S.A.P. office (Ed.), The United States of America, U.S.A, 1994, pp. 7.
[83] M. Wanlass, Systems and methods for advanced ultra-high-performance InP solar cells, in, United States, 2017.
[84] C.J. Keavney, V.E. Haven, S.M. Vernon, Emitter structures in MOCVD InP solar cells, in: IEEE Conference on Photovoltaic Specialists, 1990, pp. 141-144 vol.141.
[85] E.L. Ratcliff, B. Zacher, N.R. Armstrong, Selective Interlayers and Contacts in Organic Photovoltaic Cells, J. Phys. Chem. Lett., 2 (2011) 1337-1350.https://doi.org/10.1021/jz2002259
[86] V. Raj, T.S.d. Santos, F. Rougieux, K. Vora, M. Lysevych, L. Fu, S. Mokkapati, H.H. Tan, C. Jagadish, Indium phosphide based solar cell using ultra-thin ZnO as an electron selective layer, J. Phys. D: Appl. Phys., 51 (2018) 395301.https://doi.org/10.1088/1361-6463/aad7e3
[87] T.J. Coutts, X. Li, M.W. Wanlass, K.A. Emery, T.A. Gessert, Hybrid solar cells based on DC magnetron sputtered films of n-ITO on APMOVPE grown p-InP, in: Conference Record of the Twentieth IEEE Photovoltaic Specialists Conference, 1988, pp. 660-665 vol.661.
[88] L. Gouskov, H. Luquet, C. Gril, A. Oemry, M. Savelli, n ITO/p InP : a photo and electroluminescent diode, Revue de Physique Appliquee, 17 (1982) 125-132.https://doi.org/10.1051/rphysap:01982001703012500

[89] T.J. Coutts, N.M. Pearsall, Recent Advances in ITO/InP and CdS/InP Solar Cells, in: W.H. Bloss, G. Grassi (Eds.) Fourth E.C. Photovoltaic Solar Energy Conference, Springer Netherlands, Dordrecht, 1982, pp. 459-464.
[90] A. Subrahmanyam, V. Vasu, P. Manivannan, Studies on transport mechanism in indium tin oxide (ITO)/p-indium phosphide (InP) solar cells prepared by reactive electron beam evaporation and spray pyrolysis techniques, in: Proceedings of 1994 IEEE 1st World Conference on Photovoltaic Energy Conversion - WCPEC (A Joint Conference of PVSC, PVSEC and PSEC), 1994, pp. 1922-1925 vol.1922.
[91] X. Yin, C. Battaglia, Y. Lin, K. Chen, M. Hettick, M. Zheng, C.-Y. Chen, D. Kiriya, A. Javey, 19.2% Efficient InP Heterojunction Solar Cell with Electron-Selective TiO2 Contact, ACS Photonics, 1 (2014) 1245-1250.https://doi.org/10.1021/ph500153c
[92] K.P. Pande, C.N. Manikopoulos, ZnO・p-InP heterojunction solar cells, Solar Cells, 4 (1981) 147-152.https://doi.org/https://doi.org/10.1016/0379-6787(81)90064-8
[93] Q. Nian, K.H. Montgomery, X. Zhao, T. Jackson, J.M. Woodall, G.J. Cheng, Pulse laser deposition fabricated InP/Al-ZnO heterojunction solar cells with efficiency enhanced by an i-ZnO interlayer, Appl. Phys. A, 121 (2015) 1219-1226.https://doi.org/10.1007/s00339-015-9493-5
[94] K.H. Montgomery, Q. Nian, X. Zhao, H.U. Li, G.J. Cheng, T.N. Jackson, J.M. Woodall, Development of ZnO-InP heterojunction solar cells for thin film photovoltaics, in: 2014 IEEE 40th Photovoltaic Specialist Conference (PVSC), 2014, pp. 0524-0527.
[95] P.R. Narangari, S.K. Karuturi, Y. Wu, J. Wong-Leung, K. Vora, M. Lysevych, Y. Wan, H.H. Tan, C. Jagadish, S. Mokkapati, Ultrathin Ta2O5 electron-selective contacts for high efficiency InP solar cells, Nanoscale, 11 (2019) 7497-7505.https://doi.org/10.1039/C8NR09932D
[96] H.J. Joyce, C.J. Docherty, Q. Gao, H.H. Tan, C. Jagadish, J. Lloyd-Hughes, L.M. Herz, M.B. Johnston, Electronic properties of GaAs, InAs and InP nanowires studied by terahertz spectroscopy, Nanotechnology, 24 (2013)
[97] J. Wallentin, M.T. Borgström, Doping of semiconductor nanowires, Journal of Materials Research, 26 (2011) 2142-2156.https://doi.org/10.1557/jmr.2011.214
[98] J. Wallentin, P. Wickert, M. Ek, A. Gustafsson, L. Reine Wallenberg, M.H. Magnusson, L. Samuelson, K. Deppert, M.T. Borgström, Degenerate p-doping of InP nanowires for large area tunnel diodes, Appl. Phys. Lett., 99 (2011) 253105.https://doi.org/10.1063/1.3669697
[99] V. Raj, L. Fu, H.H. Tan, C. Jagadish, Design Principles for Fabrication of InP-Based Radial Junction Nanowire Solar Cells Using an Electron Selective Contact, IEEE J. Photovolt., 9 (2019) 980-991.https://doi.org/10.1109/JPHOTOV.2019.2911157
[100] K.V. Vidur Raj, Lily Li, Lan Fu, Hark Hoe Tan and Chennupati Jagadish, Electron selective contact for high efficiency core-shell nanowire solar cell, in: Compound Semiconductor Week 2019, Nara, japan, 2019.
[101] K.V. Vidur Raj, Lily Li, Lan Fu, Hark Hoe Tan and Chennupati Jagadish, Electron selective contact for high efficiency core-shell nanowire solar cell, in: Compound Semiconductors Week Nara, Japan 2019.
[102] P. Caban, R. Pietruszka, K. Kopalko, B.S. Witkowski, K. Gwozdz, E. Placzek-Popko, M. Godlewski, ZnO/GaAs heterojunction solar cells fabricated by the ALD method, Optik, 157 (2018) 743-749.https://doi.org/https://doi.org/10.1016/j.ijleo.2017.11.063
[103] S.-W. Kim, S.-H. Kim, G.-S. Kim, C. Choi, R. Choi, H.-Y. Yu, The Effect of Interfacial Dipoles on the Metal-Double Interlayers-Semiconductor Structure and Their Application in Contact Resistivity Reduction, ACS Appl. Mater. Interfaces, 8 (2016) 35614-35620.https://doi.org/10.1021/acsami.6b10376

[104] J. Hu, K.C. Saraswat, H.S. Philip Wong, Metal/III-V effective barrier height tuning using atomic layer deposition of high-κ/high-κ bilayer interfaces, Appl. Phys. Lett., 99 (2011) 092107.https://doi.org/10.1063/1.3633118
[105] S. Kim, G. Kim, S. Kim, J. Kim, C. Choi, J. Park, R. Choi, H. Yu, Non-Alloyed Ohmic Contacts on GaAs Using Metal-Interlayer-Semiconductor Structure With SF6Plasma Treatment, IEEE Electron Device Letters, 37 (2016) 373-376.https://doi.org/10.1109/LED.2016.2524470
[106] G. Shine, K.C. Saraswat, Limits of specific contact resistivity to Si, Ge and III-V semiconductors using interfacial layers, in: 2013 International Conference on Simulation of Semiconductor Processes and Devices (SISPAD), 2013, pp. 69-72.
[107] K. Wu, N. Song, Z. Liu, H. Zhu, W. Rodríguez-Córdoba, T. Lian, Interfacial Charge Separation and Recombination in InP and Quasi-Type II InP/CdS Core/Shell Quantum Dot-Molecular Acceptor Complexes, The Journal of Physical Chemistry A, 117 (2013) 7561-7570.https://doi.org/10.1021/jp402425w
[108] H.-V. Han, C.-C. Lin, Y.-L. Tsai, H.-C. Chen, K.-J. Chen, Y.-L. Yeh, W.-Y. Lin, H.-C. Kuo, P. Yu, A Highly Efficient Hybrid GaAs Solar Cell Based on Colloidal-Quantum-Dot-Sensitization, Sci. Rep., 4 (2014) 5734.https://doi.org/10.1038/srep05734
[109] M. Bettini, K.J. Bachmann, E. Buehler, J.L. Shay, S. Wagner, Preparation of CdS/InP solar cells by chemical vapor deposition of CdS, J. Appl. Phys., 48 (1977) 1603-1606.https://doi.org/10.1063/1.323840
[110] K.J. Bachmann, E. Buehler, J.L. Shay, S. Wagner, Polycrystalline thin-film InP/CdS solar cell, Appl. Phys. Lett., 29 (1976) 121-123.https://doi.org/10.1063/1.88964
[111] Y.W. Han, S.J. Jeon, J.Y. Choi, J.H. Kim, D.K. Moon, Highly efficient Ternary Solar Cells of 10.2% with Core/Shell Quantum Dots via FRET Effect, Solar RRL, 2 (2018) 1800077.https://doi.org/10.1002/solr.201800077
[112] S. Lin, P. Wang, X. Li, Z. Wu, Z. Xu, S. Zhang, W. Xu, Gate tunable monolayer MoS2/InP heterostructure solar cells, Appl. Phys. Lett., 107 (2015) 153904.https://doi.org/10.1063/1.4933294
[113] P. Wang, S. Lin, G. Ding, X. Li, Z. Wu, S. Zhang, Z. Xu, S. Xu, Y. Lu, W. Xu, Z. Zheng, Enhanced monolayer MoS2/InP heterostructure solar cells by graphene quantum dots, Appl. Phys. Lett., 108 (2016) 163901.https://doi.org/10.1063/1.4946856
[114] E. Singh, K.S. Kim, G.Y. Yeom, H.S. Nalwa, Atomically Thin-Layered Molybdenum Disulfide (MoS2) for Bulk-Heterojunction Solar Cells, ACS Appl. Mater. Interfaces, 9 (2017) 3223-3245.https://doi.org/10.1021/acsami.6b13582
[115] S. Saito, Y. Hashimoto, K. Ito, Ieee, Ieee, Ieee, EFFICIENT ZNO/CDS/LNP HETEROJUNCTION SOLAR-CELL, in: 1994 Ieee First World Conference on Photovoltaic Energy Conversion/Conference Record of the Twenty Fourth Ieee Photovoltaic Specialists Conference-1994, Vols I and Ii, Ieee, New York, 1994, pp. 1867-1870.
[116] D. Shahrjerdi, B. Hekmatshoar, D.K. Sadana, Low-Temperature a-Si:H/GaAs Heterojunction Solar Cells, IEEE J. Photovolt., 1 (2011) 104-107.https://doi.org/10.1109/JPHOTOV.2011.2164391
[117] S. Lin, X. Li, P. Wang, Z. Xu, S. Zhang, H. Zhong, Z. Wu, W. Xu, H. Chen, Interface designed MoS2/GaAs heterostructure solar cell with sandwich stacked hexagonal boron nitride, Sci. Rep., 5 (2015) 15103.https://doi.org/10.1038/srep15103

https://www.nature.com/articles/srep15103#supplementary-information
[118] A. Das, S. Pisana, B. Chakraborty, S. Piscanec, S.K. Saha, U.V. Waghmare, K.S. Novoselov, H.R. Krishnamurthy, A.K. Geim, A.C. Ferrari, A.K. Sood, Monitoring dopants by Raman

scattering in an electrochemically top-gated graphene transistor, Nature Nanotechnology, 3 (2008) 210.https://doi.org/10.1038/nnano.2008.67

https://www.nature.com/articles/nnano.2008.67#supplementary-information
[119] H. Xu, J. Wu, Q. Feng, N. Mao, C. Wang, J. Zhang, High Responsivity and Gate Tunable Graphene-MoS2 Hybrid Phototransistor, Small, 10 (2014) 2300-2306.https://doi.org/10.1002/smll.201303670
[120] T. Kümmell, W. Quitsch, S. Matthis, T. Litwin, G. Bacher, Gate control of carrier distribution in $k$-space in ${\mathrm{MoS}}_{2}$ monolayer and bilayer crystals, Physical Review B, 91 (2015) 125305.https://doi.org/10.1103/PhysRevB.91.125305
[121] G. Mariani, Y. Wang, R.B. Kaner, D.L. Huffaker, Hybrid Solar Cells: Materials, Interfaces, and Devices, in: X. Wang, Z.M. Wang (Eds.) High-Efficiency Solar Cells: Physics, Materials, and Devices, Springer International Publishing, Cham, 2014, pp. 357-387.
[122] J.-J. Chao, S.-C. Shiu, S.-C. Hung, C.-F. Lin, GaAs nanowire/poly(3,4-ethylenedioxythiophene):poly(styrenesulfonate) hybrid solar cells, Nanotechnology, 21 (2010) 285203.https://doi.org/10.1088/0957-4484/21/28/285203
[123] P.-L. Ong, A.I. Levitsky, Organic / IV, III-V Semiconductor Hybrid Solar Cells, Energies, 3 (2010).https://doi.org/10.3390/en3030313
[124] S. Ren, N. Zhao, S.C. Crawford, M. Tambe, V. Bulović, S. Gradečak, Heterojunction Photovoltaics Using GaAs Nanowires and Conjugated Polymers, Nano Lett., 11 (2011) 408-413.https://doi.org/10.1021/nl1030166
[125] J. Geissbühler, J. Werner, S. Martin de Nicolas, L. Barraud, A. Hessler-Wyser, M. Despeisse, S. Nicolay, A. Tomasi, B. Niesen, S. De Wolf, C. Ballif, 22.5% efficient silicon heterojunction solar cell with molybdenum oxide hole collector, Appl. Phys. Lett., 107 (2015) 081601.https://doi.org/10.1063/1.4928747
[126] J. Bullock, A. Cuevas, T. Allen, C. Battaglia, Molybdenum oxide MoOx: A versatile hole contact for silicon solar cells, Appl. Phys. Lett., 105 (2014) 232109.https://doi.org/10.1063/1.4903467
[127] S.Z. Oener, A. Cavalli, H. Sun, J.E.M. Haverkort, E.P.A.M. Bakkers, E.C. Garnett, Charge carrier-selective contacts for nanowire solar cells, Nat. Commun., 9 (2018) 3248.https://doi.org/10.1038/s41467-018-05453-5
[128] O. Pluchery, Y.J. Chabal, R.L. Opila, Wet chemical cleaning of InP surfaces investigated by in situ and ex situ infrared spectroscopy, J. Appl. Phys., 94 (2003) 2707-2715.https://doi.org/10.1063/1.1596719
[129] J.E. Webb, Simple method of making photovoltaic junctions, in: U.S.P. Office (Ed.), U.S.A, 1965.
[130] V. Raj, T. Lu, M.N. Lockrey, R. Liu, F. Kremer, L. Li, Y. Liu, H.H. Tan, C. Jagadish, Introduction of TiO2 in CuI for its Improved Performance as a p-type Transparent Conductor, ACS Appl. Mater. Interfaces, 11 (2019) 24254-24263.https://doi.org/10.1021/acsami.9b05566
[131] P. Vohl, D.M. Perkins, S.G. Ellis, R.R. Addiss, W. Hui, G. Noel, GaAs thin-film solar cells, IEEE Trans. Electron Devices, 14 (1967) 26-30.https://doi.org/10.1109/T-ED.1967.15890
[132] R.B.G. P. A. Crossley, A. Spielman, M. Wolf, Thin-film gaas photovoltaic solar energy cells, in, National Aeronautics and Space Administration, 1967.
[133] K. Cheng, H. Pan, S. Yu, W. Weng, Y. Lai, Y. Lin, Y. Chen, M. Li, H.W. Hu, P. Yu, H. Meng, 10% efficiency hybrid GaAs/PEDOT:PSS solar cells with monolayer graphene, in: 2014 IEEE 40th Photovoltaic Specialist Conference (PVSC), 2014, pp. 1519-1521.

[134] K.-F. Chang, Y.-C. Chen, K.W. Chang, M. Shellaiah, K.W. Sun, Junction model and transport mechanism in hybrid PEDOT:PSS/n-GaAs solar cells, Organic Electronics, 51 (2017) 435-441.https://doi.org/https://doi.org/10.1016/j.orgel.2017.09.044
[135] L. Yan, W. You, Orientation effect on GaAs/ultrathin polymer/PEDOT:PSS hybrid solar cell, Organic Electronics, 16 (2015) 71-76.https://doi.org/https://doi.org/10.1016/j.orgel.2014.10.037
[136] C.H. Lin, K.W. Sun, Q.M. Liu, H. Shirai, C.P. Lee, Poly(3,4-ethylenedioxythiophene):poly(styrenesulfonate)/GaAs hybrid solar cells with 13% power conversion efficiency using front- and back-surface field, Optics Express, 23 (2015) A1051-A1059.https://doi.org/10.1364/OE.23.0A1051
[137] G. Mariani, R.B. Laghumavarapu, B. Tremolet de Villers, J. Shapiro, P. Senanayake, A. Lin, B.J. Schwartz, D.L. Huffaker, Hybrid conjugated polymer solar cells using patterned GaAs nanopillars, Appl. Phys. Lett., 97 (2010) 013107.https://doi.org/10.1063/1.3459961
[138] J. Yin, D.B. Migas, M. Panahandeh-Fard, S. Chen, Z. Wang, P. Lova, C. Soci, Charge Redistribution at GaAs/P3HT Heterointerfaces with Different Surface Polarity, J. Phys. Chem. Lett., 4 (2013) 3303-3309.https://doi.org/10.1021/jz401485t
[139] M. Panahandeh-Fard, J. Yin, M. Kurniawan, Z. Wang, G. Leung, T.C. Sum, C. Soci, Ambipolar Charge Photogeneration and Transfer at GaAs/P3HT Heterointerfaces, J. Phys. Chem. Lett., 5 (2014) 1144-1150.https://doi.org/10.1021/jz500332z
[140] L. Yan, W. You, Real Function of Semiconducting Polymer in GaAs/Polymer Planar Heterojunction Solar Cells, ACS Nano, 7 (2013) 6619-6626.https://doi.org/10.1021/nn306047q
[141] K.S. Karimov, M.T. Saeed, F.A. Khalid, Z.M. Karieva, Photoconductive properties of organic-inorganic Ag/p-CuPc/n-GaAs/Ag cell, Journal of Semiconductors, 32 (2011) 072001.https://doi.org/10.1088/1674-4926/32/7/072001
[142] K.S. Karimov, M.M. Ahmed, S.A. Moiz, M.I. Fedorov, Temperature-dependent properties of organic-on-inorganic Ag/p-CuPc/n-GaAs/Ag photoelectric cell, Sol. Energy Mater. Sol. Cells, 87 (2005) 61-75.https://doi.org/https://doi.org/10.1016/j.solmat.2004.07.014
[143] R.R. LaPierre, A.C.E. Chia, S.J. Gibson, C.M. Haapamaki, J. Boulanger, R. Yee, P. Kuyanov, J. Zhang, N. Tajik, N. Jewell, K.M.A. Rahman, III–V nanowire photovoltaics: Review of design for high efficiency, Phys. Status Solidi RRL, 7 (2013) 815-830.https://doi.org/10.1002/pssr.201307109
[144] H. Borchert, Elementary processes and limiting factors in hybrid polymer/nanoparticle solar cells, Energy Environ. Sci., 3 (2010) 1682-1694.https://doi.org/10.1039/C0EE00181C
[145] R. Islam, K.C. Saraswat, Metal/insulator/semiconductor carrier selective contacts for photovoltaic cells, 2014 IEEE 40th Photovoltaic Specialist Conference (PVSC), (2014) 0285-0289
[146] F.R. Vidur Raj, Lan Fu, Hark Hoe Tan, and Chennupati Jagadish, Design of Ultra-Thin InP Solar Cell Based on Dopant Free Heterocontacts, IEEE Journal of Photovoltaics, Under Review,
[147] M. Yamaguchi, Potential and present status of III–V/Si tandem solar cells, in: 2014 IEEE 40th Photovoltaic Specialist Conference (PVSC), 2014, pp. 0821-0826.
[148] M.A. Green, Y. Hishikawa, E.D. Dunlop, D.H. Levi, J. Hohl-Ebinger, M. Yoshita, A.W.Y. Ho-Baillie, Solar cell efficiency tables (Version 53), Progress in Photovoltaics: Research and Applications, 27 (2019) 3-12.https://doi.org/10.1002/pip.3102